Reservoir Simulation of 9-Section area around Flower A1 well – Chase/Council Grove Reservoir Systems

Kansas Geological Survey

Open File Report No. – 2005-54

Authors:

Saibal Bhattacharya

Martin K. Dubois

Alan P. Byrnes

1.0 Introduction

The Hugoton and Panoma gas fields (Figure 1), North America's largest, produce from thirteen fourth-order marine-nonmarine sedimentary cycles of the Wolfcampian Chase and Council Grove Groups, respectively. A fine-layered cellular geomodel was constructed for these fields using a four step workflow: 1) define lithofacies in core and correlate to wireline log curves and geologic variables (depositional environment and relative cycle-position), 2) train a neural network and predict lithofacies at non-cored wells, 3) populate a 3D cellular model with lithofacies using stochastic methods, and 4) populate the model with petrophysical properties and fluid saturations using facies-specific equations based on core data. The fine-scale model was upscaled to 25 layers for simulation.

2.0 Objective

The objective of this study was to validate the above mentioned geomodel by simulating the production/pressure performance of wells located in select multi-Section areas in the Hugoton field. The intent of this exercise is to see how closely the simulator-calculated pressure/production performances of individual wells match with respective histories with minimum modifications of the geomodel. The focus is not to obtain exact matches of pressure/production histories at individual wells with localized model modifications. Computer Modeling Group's (CMG's) IMEX simulator was used in this study.

This report details the simulation studies carried out at one such area – 9 Section around the Flower Science well. The location of the Flower simulation within the context of the Hugoton-Panoma fields is shown in Figure 1 while Figure 2 shows the locations of the wells within this study area.

3.0 Model Inputs

3.1 Flower area geologic model

The Flower area is located near the very center of the Hugoton and Panoma gas fields where the gas column is thickest (500 feet, 150 m) and is continuous from the top of the Chase through the lower part of the Council Grove, through the Cottonwood Limestone Member (B5_LM) (Figure1). Thin-bedded (2-10 meter), marine carbonate mudstone to grainstone and siltstone to very fine sandstone siliciclastics in thirteen fourth-order marine-continental cycles, illustrated in core, are the main pay zones separated by eolian and sabkha redbeds of low reservoir quality (Figure 3.1.1). The heterolithic system is a classic example of sedimentary response to rapid glacio-eustatic sea level fluctuations on an extremely gently sloped ramp of an asymmetric foreland basin (Anadarko) on a craton. Petrophysical properties vary between eleven major lithofacies classes. Water saturations cannot be interpreted from logs due to deep filtrate invasion (Dubois et al., 2003a). Neural network procedures, stochastic modeling, and data analysis automation facilitated building a detailed 3D cellular reservoir model that is part of the Hugoton Asset Management Project (http://www.kgs.ku.edu/HAMP/index.html), a Kansas Geological Survey – industry consortium. In building the Flower static model, we used a four step workflow: 1) define lithofacies in core and correlate to electric log curves (training set), 2) train a neural network and predict lithofacies at non-cored wells, 3) populate a 3D cellular model with lithofacies using stochastic methods, and 4) populate model with lithofacies-specific petrophysical properties and fluid saturations. A portion of the static model was then upscaled for simulation

3.1.1 Reservoir Lithofacies

The main pay zones in the Hugoton consist of thirteen thin (mean thickness varying from 6-70 ft, 2 to 21 m) marine, mainly carbonate intervals (with six intervals

located in the Chase section and seven intervals located in the Council Grove section), deposited during sea level high stands. These are separated by continental, mainly siltstone (redbed) intervals (mean thickness 6-25 ft, 2-8 m) deposited during sea level low stands, when most of the shelf was exposed. The siltstones generally have poor reservoir quality and vertically isolate, or restrict communication between, the thirteen pay intervals (Seimers and Ahr 1990; Ryan et al 1994; Oberst et al 1994; Olson et al 1997). The principle factor in determining the reservoir storage and flow capacity (hydrocarbon pore volume and permeability) of Hugoton reservoir rock is primary depositional texture. Although diagenesis, both early and after burial, including leaching of grains and cements and early and late dolomitization, played important roles in enhancing or reducing porosity (Seimers and Ahr 1990; Luczaj and Goldstein 2000; Olson et al 1997), the dominant reservoir rocks are marine carbonate with grain-supported textures and, to a lesser extent, siliciclastic sandstone (Seimers and Ahr 1990; Caldwell 1991; Olson et al 1997; Hyer 1999; Dubois et al. 2003a).

3.1.2 Building the static model

For the Flower simulation exercise, a finely layered 70 square mile static model (234 layers, 1,048,320 cells) was initially built and populated with lithofacies, porosity, permeability, and water saturation (Figure 3.1.2). The xy grid dimensions are 660X660 feet (200X200 m). A nine-section portion of the model centered on the Flower A-1 well as "cut out" of the larger model and the 234-layer model was upscaled to 25 layers with porosity, permeability and water saturation for simulation.

Well data for the larger Flower area static model included formation tops from 300 wells, and facies and porosity data from 57 node wells (Figure 3.1.3). The simulation model included 6 node wells, including the Flower A1 that had a continuous core through the Chase and Council Grove. Lithofacies are estimated at half-foot (0.15 m) intervals in the 57 node wells, wells having modern log curves (density and neutron porosity, deep induction log, gamma ray, and photoelectric effect), using neural networks

trained on wells having core (Dubois et al., 2003a, 2003b, 2005). The neural network models for the Flower model are those referred to as the Geomod2 vintage neural networks. Corrected porosity at the node wells was estimated using algorithms developed from core to log porosity regression analysis (Figure 3.1.4).

3.1.3 Workflow for Static Model Construction

The following workflow was employed for building the static Flower area model:

1. Build a structural model establishing the cellular architecture based on the structural tops from the 300 wells. Model consists of 25 zones that conform to the stratigraphic nomenclature in Figure 1 and 234 conformable layers that average 2 foot (0.6 m) in the marine intervals and 4 foot (1.2 m) in the nonmarine intervals.
2. Model the lithofacies and porosity by first "blocking" the half-foot (0.15 m) data to the layered thickness at the 57 node wells using a most abundant lithofacies approach for facies and arithmetic average for porosity.
3. Model lithofacies between node wells using stochastic indicator simulation using variograms developed through data analysis.
4. Model porosity between node wells using sequential Gaussian simulation conditioned on lithofacies and using variograms developed through data analysis.
5. Water saturation was calculated at the cells using transform equations developed from empirical core data knowing lithofacies, porosity, and height above free water level.
6. Free water level was estimated to be 125 feet below the average lowest depth of perforations in the Council Grove Group.
7. Permeability in the x, y, and z directions was calculated at the cells using transform equations developed from empirical core data knowing lithofacies and porosity. Permeability x = permeability y.

3.1.4 Engineering Model

A finely-layered model is necessary to adequately distribute porosity, permeability, and water saturation in the 3D model, but is cumbersome for simulation. A 9-section portion of the 234-layer model was cut out of the larger model and upscaled to 25 layers. These layers correspond to the 25 zones in the structural model that in turn correspond to the major stratigraphic units that are marine or nonmarine half cycles. In general, the result is 25 layers that alternate from relatively good reservoir properties (higher porosity and permeability) to relatively poor reservoir properties (relatively low porosity and permeability). Porosity was upscaled using an arithmetic average, conditioned on lithofacies; water saturation was upscaled using a porosity weighted arithmetic average; and permeability upscaling utilized flow-based tensor upscaling using PSK-solver. Figure 3.1.5 illustrates the results of the upscaling from the 234-layer static model to the 25-layer engineering model. The models were exported from Petrel in a format compatible for import directly into the CMG simulator.

A 25-layer geomodel was exported to the reservoir simulator – Computer Modeling Group's IMEX. Each layer in this 25-layer model coincides with a formation- or member-level stratigraphic interval in the Chase and Council Grove systems, respectively. Each layer represents a half-cycle of marine/non-marine sedimentary cycle. In most cases, the model layer closely approximates the DST intervals at the Flower Science well. The area simulated extends over 9 Sections around the Flower Science well. Grid cells dimensions were set at 660 ft by 660 ft for all layers.

Wells have been named using an uniform convention in this study. The names of all Chase Parent wells carry a prefix "P", while those of Chase Infill and Council Grove wells carry prefixes "I" and "CG", respectively.

3.2 Permeability modeling

Fundamental to modeling the permeability distribution in the Hugoton is the need to understand the relative role of matrix and fracture flow and the possible scale dependence of permeability. Figure 3.2.1 showed that for rocks below approximately 8% porosity, or approximately 0.5 md (0.0005 μm^2), microfractures in core significantly increased permeability. A fundamental question for these data is: are the microfractures present in the subsurface or are they a stress release or coring-induced phenomenon? This question can only be answered by comparing upscaled matrix permeabilities with unfractured full-diameter permeabilities and with drill stem test (DST) or well test calculated permeabilities. Comparing carefully-examined unfractured full-diameter permeability values with that measured on plugs taken from the full-diameter cores (Figure 3.2.2) indicates that homogenous samples matrix properties apply to the full-diameter core scale.

The ability to compare well-scale permeability with matrix permeability is limited because so few wells have DST or well test data for thin intervals for which core data are available and which were tested prior to hydraulic fracturing, which complicates artificial fracture-enhanced permeability with reservoir permeability. In four key research wells, permeability was measured using DST for multiple intervals for which core analysis was also performed. To compare with core permeabilities, full-diameter and plug permeabilities were arithmetically averaged (representing parallel flow contribution from each depth interval) to determine average interval permeabilities. Correlation between DST, upscaled full-diameter, and plug permeabilities shows good correlation for intervals with permeability greater than ~0.5 md (0.0005 μm^2). For interval permeabilities below 0.5 (0.0005 μm^2) md, full-diameter permeabilities exhibit nearly constant permeability between 0.5 and 3 md (0.0005-0.000033 μm^2), characteristic of microfracture-influenced permeability. Matrix-scale plug permeabilities are both higher and lower than DST permeabilities (Figure 3.2.3).

Variance in the DST-matrix correlation is partially or predominantly related to the limited vertical sampling of the core plugs and difficulty in representing some pore properties that are larger in scale than core plugs. The single phylloid algal bafflestone interval exhibits significantly lower matrix permeability because core plugs did not sample the larger-scale vuggy nature of this lithofacies, which exhibits high permeability. Since microfractures do not contribute significantly to measured permeability for rocks with permeability greater than 0.5 md (0.0005 μm^2), both full-diameter and plug data reflect matrix properties and the good correlation with DST permeabilities indicates that the reservoir is not fractured at the scale of investigation of the DST test. The better correlation of plug and DST permeabilities for intervals with permeability below 0.5 md, and the fact that upscaled permeabilities from plug data are greater than or equal to DST permeabilities, for three of the four intervals, can be interpreted to indicate that these intervals are also unfractured. These data, and less precise data from other wells, indicate that the production characteristics of many wells in the Hugoton are consistent with matrix properties without significant natural fracture contribution. Data and statistics on the fraction of wells that exhibit production greater than what would be predicted from matrix properties have not yet been compiled and calculated.

Facies-specific permeability-porosity co-relationships were used for an initial estimate of grid permeabilities in each layer. Layer-DSTs from the Flower well were interpreted to estimate layer permeabilities effective in the drainage area of the science well. Also, permeabilities were measured at intervals of half-feet along the length of the Chase and Council Grove core retrieved from the Flower well. The core-derived (horizontal) permeability values at half-foot intervals were arithmetically averaged (upscaled) to derive the layer (horizontal permeability).

The geomodel built in Petrel® consisted of 69 layers. The tensor upscaling algorithm in Petrel® was used to upscale vertical and horizontal permeability to 25-layers before exporting the model to CMG. For each layer at the place of location of the Flower Science well, the upscaled permeability was compared with that calculated from DST. For most layers the upscaled permeability was found to be close to that calculated from

DSTs. For layers where the upscaled permeability differed from DST-permeability, an appropriate multiplier was applied so that the layer permeability matched that calculated from the DST. For each layer, Table 3.2.1 summarizes the initial upscaled permeability and the multiplier applied to each layer so that the layer-permeability matched permeability derived from DST.

3.3 Reservoir pressure

The first recorded surface shut-in (SI) pressures (soon after completion) at the Chase Parent wells in the area studied varied between 361 to 422 psi (Table 3.3.1). The well head shut-in pressure for the first CHP well drilled in the study area (Zimmerman 1) was 422 psi while that at the last CHP well (Betts 1) was 361 psi. Surface shut-in pressures have to be converted to bottom-hole shut-in pressures. Table 3.3.2 shows the estimation of initial reservoir pressure from recorded surface shut-in pressures following the average temperature and z-factor method. The estimated initial reservoir pressure is about 460 psi assuming a WHSP of 422 psi. Thus, initial simulation runs were carried out using starting reservoir pressure of 460 psi which resulted in charging the input geomodel (for the area studied) with an original-gas-in-place (OGIP) of 196 bcf.

3.4 Hydraulic Fractures

All wells in the study area had been fractured. The Chase Infill and the Council Grove wells were fractured upon completion. The Chase Parent wells were drilled before fracturing technology was developed and thus produced un-fractured until the 1960s. The exact dates of hydraulic fracturing the Chase Parent wells are not known. Thus, all Chase Parent wells have been assumed to be fractured on January 1960. This date approximately coincides with a visible increase in production from the Chase wells. However, there is no information or test data available which would enable one of estimate the physical characterization of these fractures. The intent of the fracturing was

to enhance the well productivity. Lacking physical descriptions of hydraulic fractures, the enhanced well productivities were modeled in this study using the well productivity (ff) factor greater than 1 with the ff set to 1.0 for an un-fractured well.

Limited pressure test data were available for Alexander D2 well located outside the study area. An approximate estimation of fracture half-length was made by analyzing this data. Sensitivity studies were carried out at individual wells in the study area by modeling the fractures with local grid-refinements using half-lengths from Alexander D2. The effects of hydraulic fractures defined by local grid refinement were replicated when ff = 6.0 was used at respective wells. Thus, each well was assigned an ff = 6.0 to model it flow behavior after hydraulic fracturing.

In this study, ff values ranging between 4 and 9 resulted in history matches at most Chase wells with minimal excess flow capacity when wells were freed of rate-constraints. That hydraulic fractures resulted in an increase in well productivity by 4 to 9 times an un-fractured well was found acceptable by operators of the field.

3.5 Flow Constraints

Monthly production data were available for all wells except the Chase Parent wells for which annual production were available for years before 1953 and bi-annual cumulative production was available from 1953 to 1966. From 1967 onwards, monthly production data were available for the Chase Parent wells. Regular tubing head flow and shut-in pressure data were available for all wells from 1967 onwards.

All wells were flowed under rate constraints until June 2003. Thereafter, all wells were flowed under a constant bottom-hole pressure (BHP) of 14.7 psi till December 2004. The intent of changing from rate constraint to pressure constraints was to see if the simulator-calculated production rates from July 2003 followed the already established decline trends without showing production spikes (or signs of excess flow capacity).

4.0 Reservoir Simulation Studies

4.1 RUN 1

The initial simulation runs were carried out by confining the completion of Chase (CH) wells within the Chase layers and those of the Council Grove (CG) wells in the CG layers. Figures 4.1.1 to 4.1.3 show the result of the resulting history matches obtained at the Chase Parent (CHP), Chase Infill (CHI), and CG wells. The ff factor was set to 6 for all wells except the PTrot24 (Trotter 1-24) Production is matched at all CHP wells with the simulator-calculated bottom hole flowing pressure (BHFP) closely matched the trend of the well-head-flowing-pressure (WHFP). Though a regular record of well-head-shut-in-pressures (WHSP) was available, field operators expressed doubts whether the recorded WHSP (after 72-hrs of SI) was stabilized to be representative of the reservoir conditions and about the procedure to convert tubing head pressures to reservoir conditions. It was thus recommended that the simulator-calculated bottom hole flowing pressures be matched against the flowing pressures recorded at the surface taking into cognizance the fact that a small discrepancy was expected to be present between flowing surface and bottom hole pressures. A production spike was observed in most CHP wells after the wells were flowed free of rate constraints in July 2003 indicating presence of excess flow capacity.

Figure 4.1.2 shows the history matches obtained for CHI wells. Production matches were obtained at all wells except IPer (Persinger) which is a border well. The simulator-calculated BHFPs are significantly higher than the corresponding WHFPs. Production spikes are visible after wells are released from rate constraints indicating presence of excess flow capacity. Figure 4.1.3 shows the history matches obtained for the CG wells. With CG completions constrained to CG layers, simulator-calculated production rates could not match the historic values at any of the CG wells. Figure 4.1.4 shows the simulator-calculated pressure distribution as of January 1970, i.e., just before the CG wells came online. The simulator output indicates that the CG layers are at 460 psi. However, initial surface SI pressures at all CG wells before onset of significant

production converge to 265 psi. Adjusted for gas column, this SI pressure translates to around 280 psi.

Between the start of production in the 1930s and 1940s and January 1970, the CHP wells have been on production and this resulted in lower pressures in the CH layers. Figure 4.1.4 indicates that the simulator results show differential depletion in the CH layers with Layer 2 (i.e. Krider) being at 285 psi. Thus for CG wells to show initial SI pressures in the range of 280 psi, one possibility is to extend the CG well completions into Chase layers. But this brings forth the question as to how far into CH do the CG well completions need to extend. It appears from the pressure distribution in Figure 4.1.4 that if the CG completions were extended to Layer 2 then upon SI the test will straddle all CG layers (which are above 400 psi) and most of CH layers one of which (i.e., Layer 2) is at 285 psi. The test of this assumption is to rerun the simulation with CG completions extending to Layer 2 and then analyze the simulation output to see if the CG wells record SI pressures around 280 psi upon completion and also that the simulator-calculated production rates at CG wells match those recorded historically.

4.2 RUN 2

Completions in CG wells were extended to Layer 2 (Krider). Figure 4.2.1 shows the history matches for CHP wells. The simulator-calculated rates matched historic rates in all wells, and thus extending CG completions into Krider did not interfere with production from the CHP wells. The simulator-calculated BHFP and the recorded WHFPs are close and follow similar trends. Figure 4.2.2 compares the simulator-calculated flow rates with historic rates for the CHP wells. Upon release from rate constraints in July 2003, most wells except Persinger (PPer) show a production spike indicating the presence of excess flow capacity due to high ff values and/or excess OGIP. Figure 4.2.3 displays the history matches obtained for the CHI wells. Cumulative production is matched at all wells except Persinger (IPer), which is a border well. Thus, extending completions of CG wells to Krider (Layer 2) did not disturb the production

matches at the CHI wells. The simulator-calculated BHFP is higher than the recorded WHFP in most non-border wells. The BHFP trends are similar to that of WHFP before flattening in later flow periods indicating excess flow capacity (i.e. too high ff and/or OGIP). Figures 4.2.4a and 4.2.4b show the history matches obtained for the CG wells. The cumulative production is matched in all CG wells. The BHFP is slightly higher than WHFP in most wells. However, the BHFP trends are similar to WHFP initially before flattening during the later flow period indicating excess flow capacity.

It appears from the above simulation runs that ff = 6 is perhaps too high for most CHP, CHI, and CG wells because of the presence of a production spike in July 2003 and a flattening of the simulator-calculated BHFP in the later part of the flow period. Thus, selective reduction in ff was carried out in most CHP wells. Simulation runs were carried out with ff = 2 and 3 for CHP wells. However, such reduction in ff was not effective in doing away with the production spikes. Any further reduction in ff values in order to eliminate the production spikes would mean that hydraulic fracturing either did not improve well productivity or improved it by a minor fraction. As mentioned earlier, field operators were comfortable with the assumption that hydraulic fracturing resulted in a significant increase in well productivity such that an assumption of ff = 6 (or around 6) can be considered reasonable.

The presence of excess flow capacity can be attributed to multiple factors and/or any combination of them. Important factors that contribute to well flow capacity include: a) ff value, b) OGIP in the drainage area, and c) effective permeability distribution in drainage area. The above discussed simulation runs were carried out assuming that the initial reservoir pressure in the Flower study area was 460 psi (resulting in OGIP = 196 bcf) based on the initial surface SI pressure of 422 psi at one CHP well, the Zimmerman 1 (Table 3.3.1). The surface shut-in pressure of 422 psi is at best reflective of the conditions prevailing within the drainage area of the Zimmerman 1 well. It is reasonable that production from other CHP wells drilled earlier or contemporary to Zimmerman 1 to have affected the average reservoir pressure in the Flower study area. Thus, the problem of excess flow capacity may be caused due to assuming a high initial reservoir pressure,

i.e. 460 psi. Also, given the heterogeneity in reservoir permeability it is quite possible that there was some variation (within a range) in the initial reservoir pressure over the study area.

To address the problem of excess flow capacity, the following simulation runs were carried out by assuming a lower initial reservoir pressure, i.e., 435 psi which results in an OGIP of 185 bcf.

4.3 RUN 3

The initial reservoir pressure was set at 435 psi and completions of CG wells were extended to Krider (Layer 2) in this run. Figure 4.3.1 shows the history matches obtained for the CHP wells when ff values were set between 5 and 9. Production was matched at all CHP wells. Only the PBet (Betts) well show a small production spike (compared to previous runs) when produced free of rate constraints. Figure 4.3.2 compares the simulator-calculated BHFPs with the recorded WHFPs. A close match is observed for all the CHP wells. Figure 4.3.3a and 4.3.3b show the history matches obtained at CG wells. Production is matched for all CG wells and 3 wells do not show any production spikes upon release from rate constraints. Presence of production spikes in remaining CG wells is indicative of ff adjustments.

4.4 RUN 4

Figures 4.4.1a and 4.4.1b show the history matches for the CG wells when ff values in wells showing production spikes (in Run 3) are adjusted (reduced from the initial value of 6). Despite reduction of ff value to between 2 and 3, production spikes remain in the CG wells. It appears that ff values must be reduced below 2 to reduce/eliminate the remaining production spikes. Thus, it appears that the production spikes are perhaps a result of

excess OGIP rather than high ff values. Hence, the initial reservoir pressure was reduced to 423 psi (resulting in an OGIP of 179.5 bcf) for the following runs.

4.5 RUN 5

Figure 4.5.1 shows the history matches for CHP wells. Simulator-calculated well production rates match with historic rates and production spikes are eliminated (or significantly reduced) with minor adjustments to ff values in select wells. Figures 4.5.2a and 4.5.2b summarize the history matches obtained for the CG wells. Some wells still show production spikes and thus the following run incorporates ff adjustments especially for select CG wells.

4.6 RUN 6

Figure 4.6.1 shows the history matches at CHP wells whose ff values vary between 5 and 9. The above figure depicts good history match of production rates at the CHP wells with minimal or no production spikes. Figure 4.6.2 depicts a good match between the simulator-calculated BHFPs and the recorded WHFPs at CHP wells. Figure 4.6.3a and 4.6.3b display the match between simulator-calculated production and historic rates for CG wells with ff values set between 5 and 9. Production rates are matched at all CG wells during flow under rate constraints. Some CG wells still show a production spike when flowed free of rate constraints. However, the magnitudes of these remaining production spikes are significantly less than previous runs. Figures 4.6.4a and 4.6.4b compares the simulator-calculated BHFPs with the recorded WHFPs. The pressure values closely follow similar decline trends. Figure 4.6.5 production history matches for the CHI wells. Production is matched at CHI wells that are not located close to the border of the area simulated. It is reasonable to expect a lack of match at these border wells, marked by red boxes, since part of the area drained by these wells lies outside the area simulated. Also, no significant production spikes are visible at the non-border wells. Figure 4.6.6 compares the simulator-calculated BHFPs with recorded WHFPs. The pressure values for

the non-border wells closely follow similar trends. However at some of the wells, the simulator-calculated pressures flatten at later flow periods, which may indicate excess flow capacity. As expected, pressure matches are absent for the border wells.

Figure 4.6.7 displays the simulator pressure distribution in each layer as of January 1, 1970 – i.e., just prior to the drilling of the CG wells in the study area. The reservoir pressure in Krider (Layer 2) is around 250 psi, while it ranges between 350 and 380 psi for the other CH zones. As noted earlier, CG wells in the study area tested surface shut-in pressures around 265 psi upon completion. Thus to test the robustness of the reservoir model being simulated, a hypothetical CG well was placed at the center of the study area (Figure 4.6.8A) and its completion extended from Krider (Layer 2 in Chase) to B5Lime (Layer 23 in Council Grove) – similar to other CG wells in this model. This test well was named "SI Well", and was completed within the simulator input file on January 1, 1970. Available records do not clearly indicate if the initial shut-in tests at the CG wells were carried out before or after the hydraulic fracturing. Thus, ff values at this well were maintained at 1. Local grids around this test well were subjected to refinement to reduce grid-size induced errors in calculated build-up pressures. The well was flowed for a day within the simulator and then shut-in for 72 hours (following the field practice in the 1970s at the time of drilling of the CG wells). The SI pressure at this test well was found to stabilize around 238 psi (Figure 4.6.8B).

The Flower Science well was drilled in early 1995, and detailed layer-specific DST recordings are available from this test well. Figure 4.6.9 displays the simulator-calculated pressure distribution in layer as of January 1, 1995. Figures 4.6.10A and 4.6.10B compare the simulator-calculated layer pressure at the location of the Flower Science well with that recorded in the field by DSTs carried out in early 1995. Close matches were obtained in most layers except L/FTRLY, B2LM, and B4LM where the simulator-calculated pressures were significantly higher than that recorded in DSTs. Thus despite matching production histories at the CG wells, layers such as B2LM and B4LM in this simulation model did not drain to the extent suggested by the Flower DSTs. The question that naturally arises at this juncture is if gas from the above two CG layers is

being drained by non-CG wells, i.e., CH wells. Such a situation would be possible if completions at the CHP and CHI wells extended into the CG layers. Thus in the succeeding simulation runs, completions at the CHP and CHI wells were extended to Layer 23 (i.e. B5 Lime/Shale) while completions at the CG wells remained extended to Layer 2 (Krider).

4.7 RUN 7

Completions at the CHP and CHI wells have been extended to Layer 23 (B5 Lime/Shale). Production and pressure matches at the CHP, CHI, and CG wells remain unchanged. Within the simulator model, a hypothetical CG well was located at the center of the study area (Figure 4.7.1A) and completed on January 1, 1970. A 72-hr shut-in was carried out at this hypothetical CG well in January 1970 resulting in a shut-in pressure of 256 psi (Figure 4.7.1B). This simulator-calculated shut-in pressure at the CG well upon completion is closer to 265 psi – the surface pressure recorded at most CG wells in the study area upon completion. Thus, extending the CH fractures into CG results in shut-in pressures closer to that recorded in the field at CG wells upon their completion. Figure 4.7.2 compares the simulator-calculated layer pressures at the Flower Science well from Run 6 (Figure 4.7.2B) and Run 7 (Figure 4.7.2C) as of January 1995 with that recorded by DST. Extending completions at the CH wells into CG while CG completions extend into Chase appears to improve the layer pressure matches at the Flower Science well. Also, such a model results in a simulator-calculated SI pressure at a hypothetical CG well to come closer to 265 psi while not compromising the production and pressure history matches at CHP, CHI, and CG wells.

Figure 4.7.3 compares the simulator-calculated layer pressure values at the Flower Science as of January 1, 2004, with that calculated as of January 1, 1995, to highlight layers that significantly contribute to the production between 1995 and 2004. Figure 4.7.4 compares the simulator-calculated reservoir pressures, in each layer (Chase and Council Grove) at the location of the Flower Science well between January 1995 and January

2004. This plot clearly shows that per the current model, greater pressure declines occur in the Chase layers as compared with the Council Grove layers. Thus, most of the production, harvested by the existing wells in the study area (i.e., CHP, CHI, and CG wells) over the above mentioned decade, originates from the Chase layers.

Figure 4.7.5 displays as a 3D-volume the simulator-calculated pressure distribution in the study area as of January 1, 2004. The area modeled in this study is assumed to produce under volumetric expansion. Thus, external fluids (water) do not influx into the study area volume. Hence, gas saturations do not change over time. Continued production from the wells results in changes in reservoir pressure depending on the gas volumes contributed by a layer or any local reservoir volume. Remaining potential, therefore, lies in areas where remaining high pressures (as of January 1, 2004) combine with better porosity, pay thickness, and effective permeability. Layers with high remaining pressures will not be prospective if their porosity, pay thickness, and effective permeability are low. Recovery volumes from future wells also depend on the type of completions, i.e., if the well is vertical or horizontal connecting one or more layers.

4.8 RUN 8

This simulation run looks at a "what if" scenario – What happens if completions in CH wells extended to B2LM (Layer 17) rather than B5LM (i.e. Layer 23) while the completions at the CG wells extended to FTRLY (i.e. Layer 8) rather than Krider (i.e. Layer 2)? Results from this simulation run show that production matches were obtained at CHP and CHI wells. However, production spikes surfaced in case of some of these CH wells when wells flowed free of rate constraints. Also, the simulator-calculated production rates at the CG wells fall short of recorded rates (Figure 4.8.1). Figure 4.8.2 compares the simulator-calculated layer pressure data at the location of the Flower Science well from Run 7 with that from Run 8. In Run 8, the simulator-calculated production rates for CG wells fell short of recorded history while Run 7 resulted in good

matches. The above figure indicates that based on the current reservoir model, completions at the CG wells have to extend up and into the Chase beyond FTRLY.

5.0 Conclusions

a) Increasing OGIP in CG layers within petrophysical constraints while using a permeability distribution that mirrors layer permeability calculated from DSTs recorded at the Flower Science well does not result in production history matches at CG wells.

b) Production matches at the CG wells are achieved only when CG wells communicate with CH gas. In this study, such communication was established by extending completions at the CG wells into CH layers.

c) CG completions need to extend up to Krider (in Chase) for CG wells to show an intial SI pressure in the vicinity of 265 psi upon well completion in January 1970.

d) An OGIP of 180 bcf (spread between the CH and CG layers) is sufficient to obtain production/pressure matches at the CH and CG wells using ff values between 5 to 9. Such a model, also, resulted in minimal or no production spikes when wells are set free of their rate constraints and produce under pumped off conditions.

e) Extending CH completions into B5LM (i.e. into CG) while completions in the CG wells extended into Krider (i.e. into CH) improved the match (as of January 1995) between the simulator-calculated layer pressure at the location of the Flower well with that recorded from DST. It also resulted in a closer match between the simulator-calculated SI pressure at a hypothetical CG well, located in the center of the study area, that recorded at CG wells upon completion in the study area

f) Run 7 provided the best match with all available pressure and production data in the study area including:

i) Production history matches at CHP, CHI, and CG wells

ii) Close match between simulator-calculated BHFPs and recorded WHFPs at CHP, CHI, and CG wells

iii) Minor or no production spikes at the above mentioned wells when they were flowed under pumped off conditions and free of rate constraints.

iv) SI pressures close to 265 psi at a hypothetical CG well upon completion in January 1970.

v) Good match of simulator-calculated layer pressures at the Flower Science well with that recorded by DSTs as of January 1995

vi) ff values for most wells cluster around 6.

g) Extending CH completions to B2LM while extending CG completions to FRTLY does not result in production history matches at the CG wells.

REFERENCES

Caldwell, C. D., 1991, Cyclic Deposition of the Lower Permian, Wolfcampian, Chase Group, Western Guymon-Hugoton Field, Texas County, Oklahoma, in Midcontinent Core Workshop: Integrated Studies of Petroleum Reservoirs in the Midcontinent: Midcontinent American Association of Petroleum Geologists Section Meeting, Wichita, Kansas, p. 57-75.

Dubois, M. K., A. P. Byrnes, G. C. Bohling, S.C. Seals, and J.H. Doveton, 2003, Statistically-based lithofacies predictions for 3-D reservoir modeling: examples from the Panoma (Council Grove) Field, Hugoton Embayment, Southwest Kansas (abs): Proceedings AAPG 2003 Annual Convention, Salt Lake City, Utah, v.12, p. A44, *and* Kansas Geological Survey Open File Report #2003-30, 3 panels, http://www.kgs.ku.edu/PRS/publication/2003/ofr2003-30/index.html (accessed October 10, 2005).

Dubois, M.K., G.C. Bohling, A.P. Byrnes, and S.C. Seals, 2003, Extracting Lithofacies from Digital Well Logs Using Artificial Intelligence, Panoma (Council Grove) Field, Hugoton Embayment, Southwest Kansas, (abs) Mid-continent Section AAPG Meeting, Tulsa, *and* KGS Open-file Report 2003-68, http://www.kgs.ku.edu/PRS/publication/2003/ofr2003-68/index.html (accessed December 21, 2005).

Dubois, M. K., A. P. Byrnes, and G. C. Bohling, 2005, Geologic model for the giant Hugoton and Panoma fields: (abs) AAPG Midcontinent Section Meeting, Oklahoma City, Oklahoma, http://www.kgs.ku.edu/PRS/Poster/2005/MidcontAAPG/index.html (accessed October 10, 2005).

Heyer, J. F., 1999, Reservoir characterization of the Council Grove Group, Texas County, Oklahoma, *in* D.F. Merriam, ed., Transactions of the American Association of Petroleum Geologists Midcontinent Section Meeting, Wichita, KS, p. 71-82.

Luczaj, J. A., and R. H. Goldstein, 2000, Diagenesis of the Lower Permian Krider Member, southwest Kansas, U.S.A.: fluid-inclusion, U-Pb, and fission-track evidences for reflux dolomitization during latest Permian time, Journal of Sedimentary Research, vol. 70, no. 3, p. 762-773.

Oberst, R. J., P. P. Bansal, and M. F. Cohen, 1994, 3-D reservoir simulation results of a 25-square mile study area in Kansas Hugoton gas field: Paper SPE 27931, SPE Mid-Continent Gas Symposium, Amarillo, Tx., p. 137-147.

Olson, T. M., Babcock, J. A., Prasad, K. V. K., Boughton, S.D., Wagner, P.D., Franklin, M.K., and Thompson, K.A., 1997, Reservoir characterization of the giant Hugoton Gas

Field, Kansas, American Association of Petroleum Geologists Bulletin, v. 81, p. 1785-1803.

Ryan, T. C., M. J. Sweeney, and W. H. Jamieson Jr., 1994, Individual layer transient tests in low-pressure, multi-layered reservoirs: Paper SPE 27928, SPE Mid-Continent Gas Symposium, Amarillo, Texas, p. 99-113.

Siemers, W. T., and W. M. Ahr, 1990, Reservoir facies, pore characteristics, and flow units: Lower Permian Chase Group, Guymon-Hugoton Field, Oklahoma, Society of Petroleum Engineers proceedings 65th Annual Technical Conference and Exhibition, New Orleans, LA, September 23-26, 1990, p. 417-428, SPE #20757.

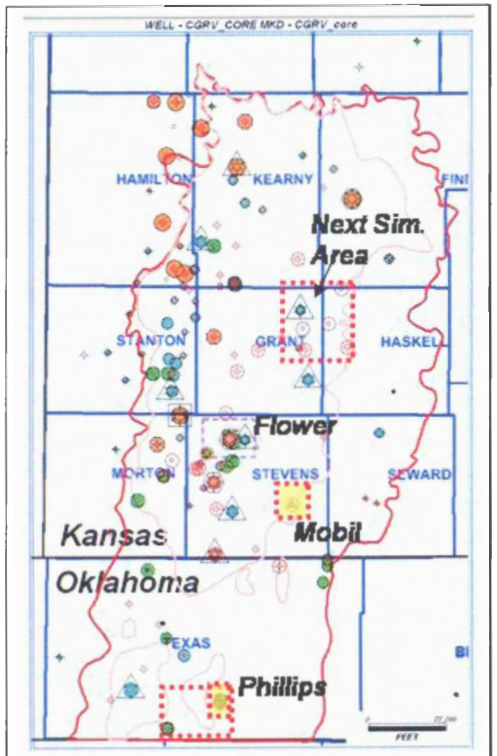

Hugoton-Panoma - 25 wells with P by zone are circled (05/10/05). Wolfcamp cores are colored (Blue=CGRV, Green=CHSE, Orange=Both)

Figure 1.

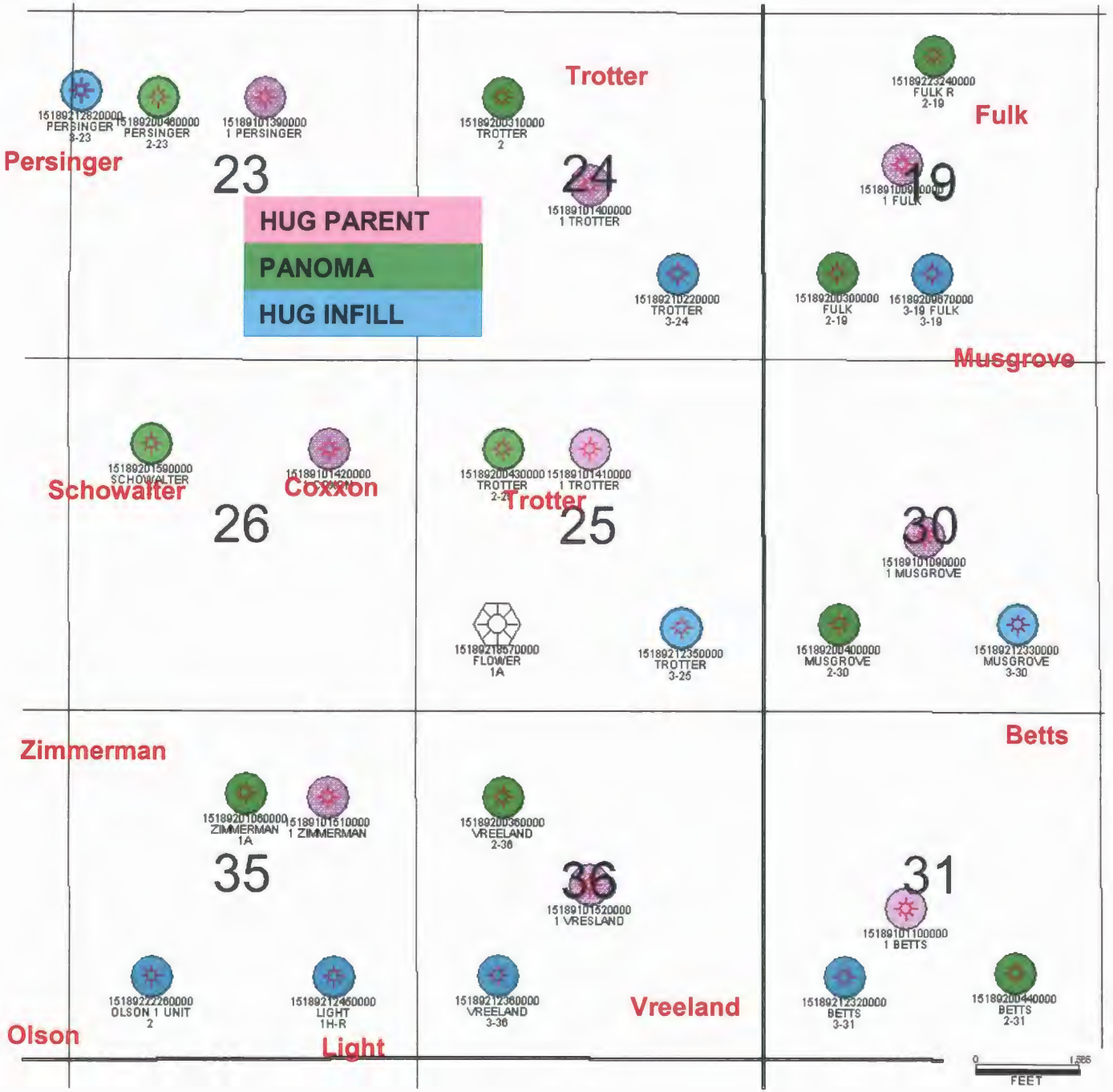
HUG PARENT
PANOMA
HUG INFILL
Persinger
Trotter
Fulk
Musgrove
Schowalter
Coxxon
Trotter
Zimmerman
Betts
Olson
Light
Vreeland
23
24
19
26
25
30
35
36
31
15189212820000 PERSINGER 3-23
15189200460000 PERSINGER 2-23
15189101390000 1 PERSINGER
15189200310000 TROTTER 2
15189101400000 1 TROTTER
15189210220000 TROTTER 3-24
15189223240000 FULK R 2-19
15189100900000 1 FULK
15189200300000 FULK 2-19
15189200870000 3-19 FULK 3-19
15189201590000 SCHOWALTER
15189101420000
15189200430000 TROTTER 2-25
15189101410000 1 TROTTER
15189101090000 1 MUSGROVE
15189218570000 FLOWER 1A
15189212350000 TROTTER 3-25
15189200400000 MUSGROVE 2-30
15189212330000 MUSGROVE 3-30
15189201060000 ZIMMERMAN 1A
15189101610000 1 ZIMMERMAN
15189200360000 VREELAND 2-36
15189101520000 1 VRESLAND
15189101100000 1 BETTS
15189222260000 OLSON 1 UNIT 2
15189212460000 LIGHT 1H-R
15189212360000 VREELAND 3-36
15189212320000 BETTS 3-31
15189200440000 BETTS 2-31
0
1,566
FEET

Figure 2.

Flower A-1 well, Sec 25-31S-38W, Stanton County, Kansas. Formation and members of the Chase and Council Grove Groups (Permian, Wolfcampian) that are shown are generally half-cycles of stacked – marine-nonmarine cycles. Lithofacies 3-10 are marine and 0-2 are nonmarine (continental).

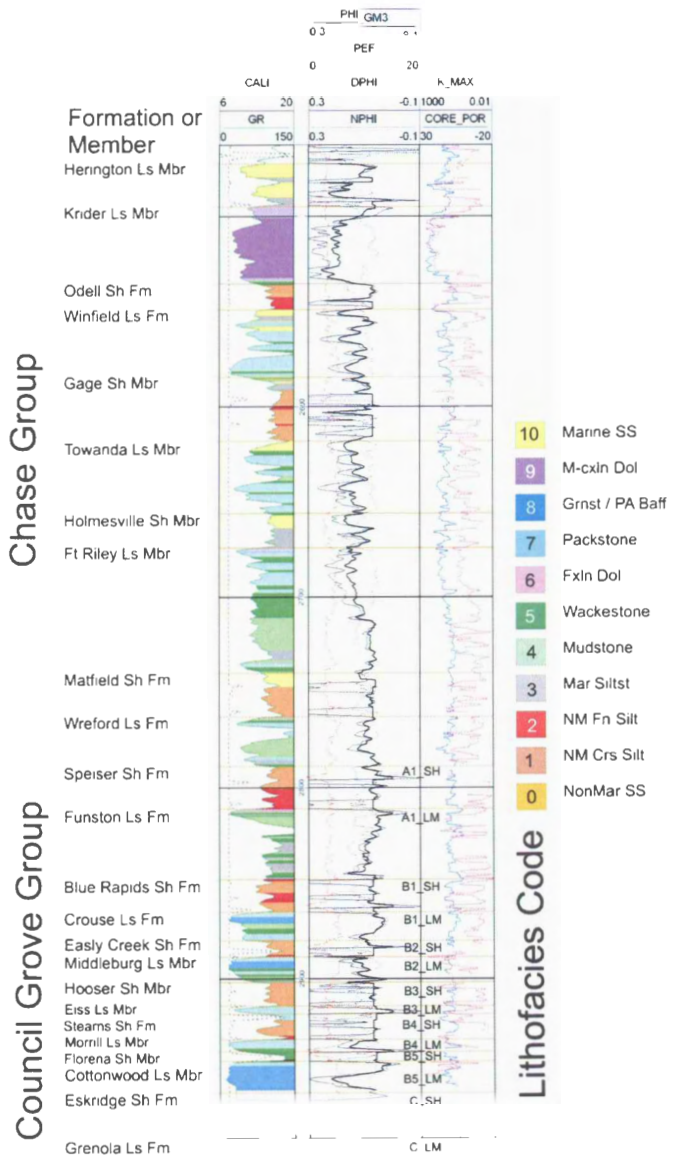

Figure 3.1.1

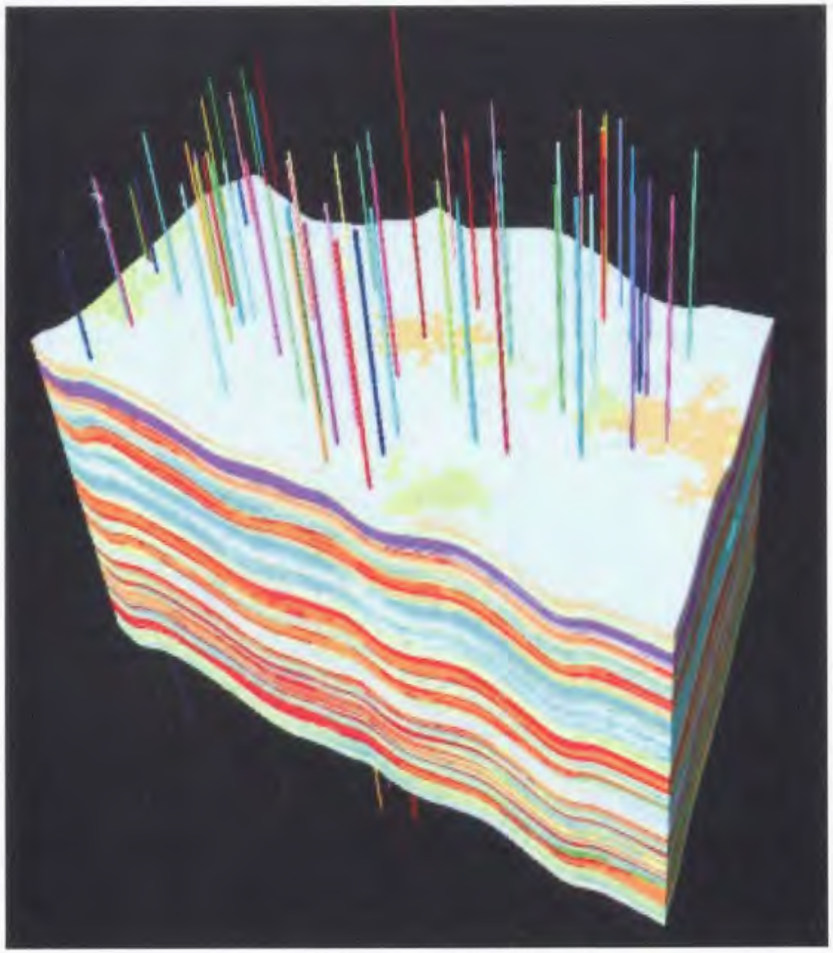

Flower area static model. Color coded lithofacies in the 70 square mile, 234-layer, static model are illustrated. Wells with facies and porosity information are shown (node wells).

Figure 3.1.2

Well data for the larger Flower area static model included formation tops from 300 wells, facies and porosity data from 57 node wells. The simulation model (shaded green) included 6 node wells, including the Flower A1 that had a continuous core through the Chase and Council Grove. The Newby well has continuous core in the Council Grove.

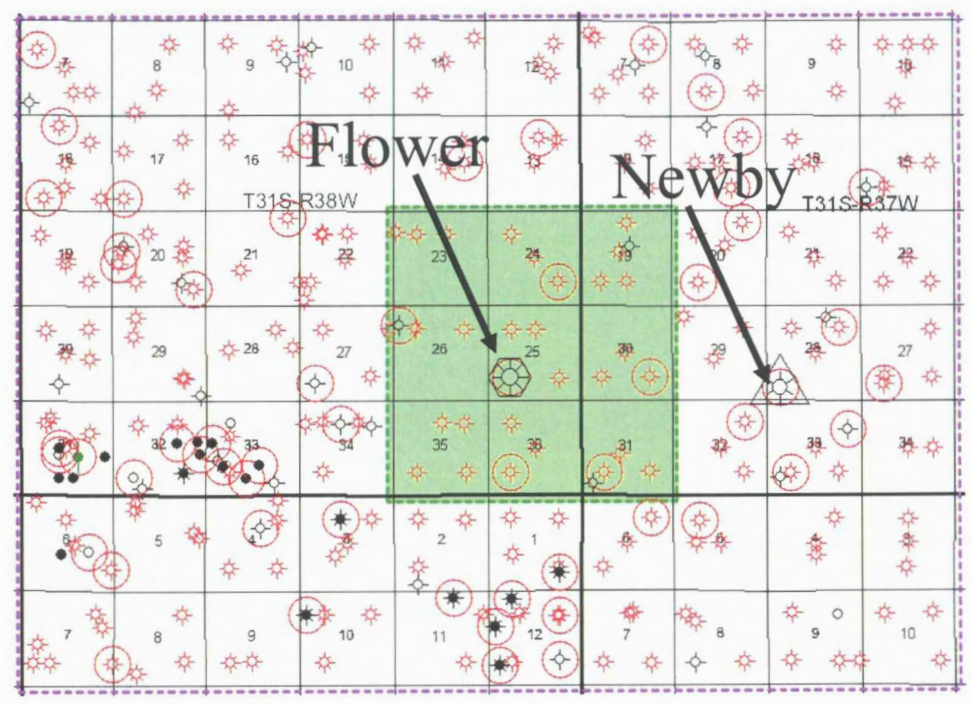

Figure 3.1.3

$$PHI\_CORR = A + B*DPHI + C*NPHI$$

	Intercept A	PHID B	PHIN C
Facies 1 & 2	0.018	0.843	0.000
Facies 3 & 4	0.019	0.662	0.000
Facies 5 & 7 & 8	4.278	0.400	0.209
Facies 6	0.000	0.500	0.500
Facies 9	8.918	0.447	0.131
Facies 10	4.484	0.524	0.135

Regression analysis of core to log porosity results in an equation and set of constants by lithofacies.

Figure 3.1.4

Properties in static and upscaled models shown in intersecting EW (25-layer upscaled) and NS (234-layer static model) that intersect at the Flower A1 well. Well trajectories are shown for the node wells.

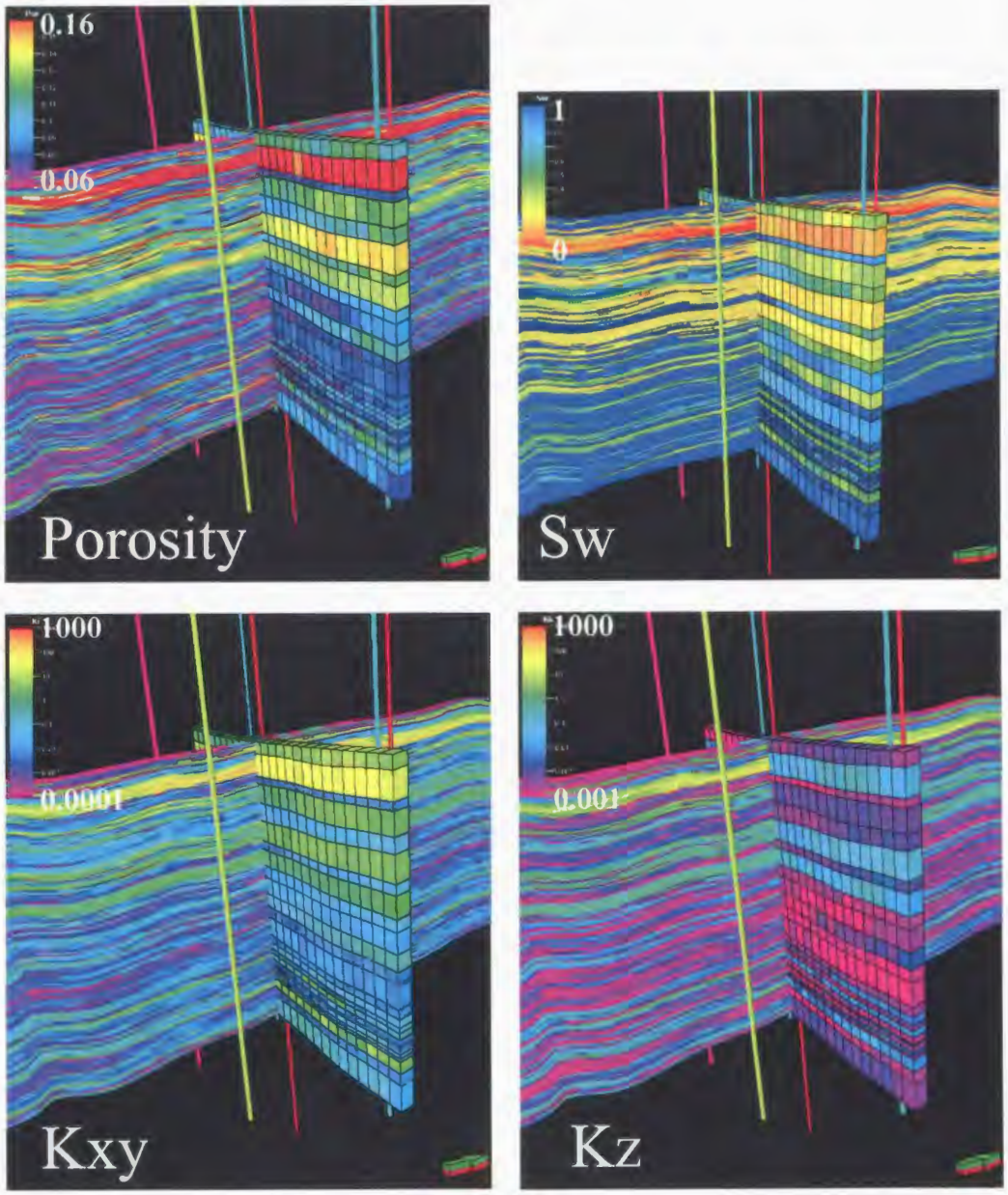

Figure 3.1.5

Crossplot of *in situ* Klinkenberg permeability versus *in situ* porosity for whole core identified as fractured (asterisks), whole core that were not identified as fractured but may contain microfractures (grey circle), and unfractured core plugs (black triangle). Permeabilities shown were either measured or routine values were corrected to *in situ* conditions using the equation presented in Figure ALAN2. Whole core (full-diameter) values diverge from matrix (plug) values at porosities less than ~10%. This can be interpreted to indicate the dominant influence of microfracture(s) on permeability in whole core samples with porosity < 10% and corresponding permeability < ~0.5 md. Above 10 % porosity influence of microfracure(s) is small.

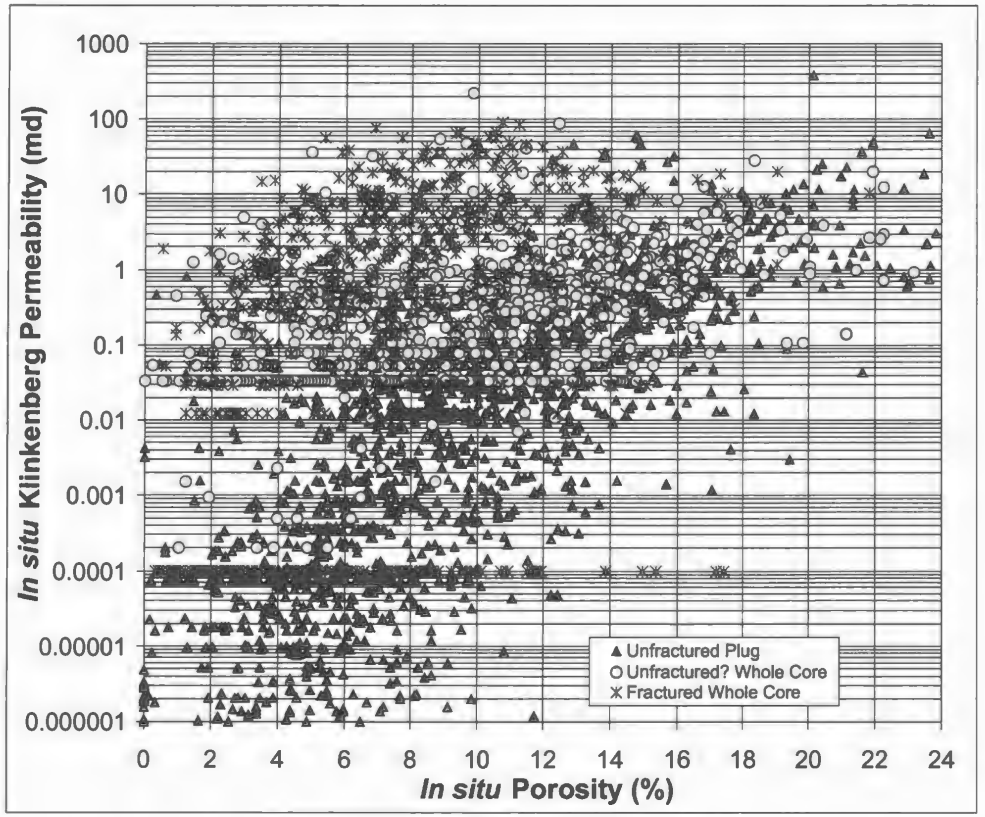

Figure 3.2.1

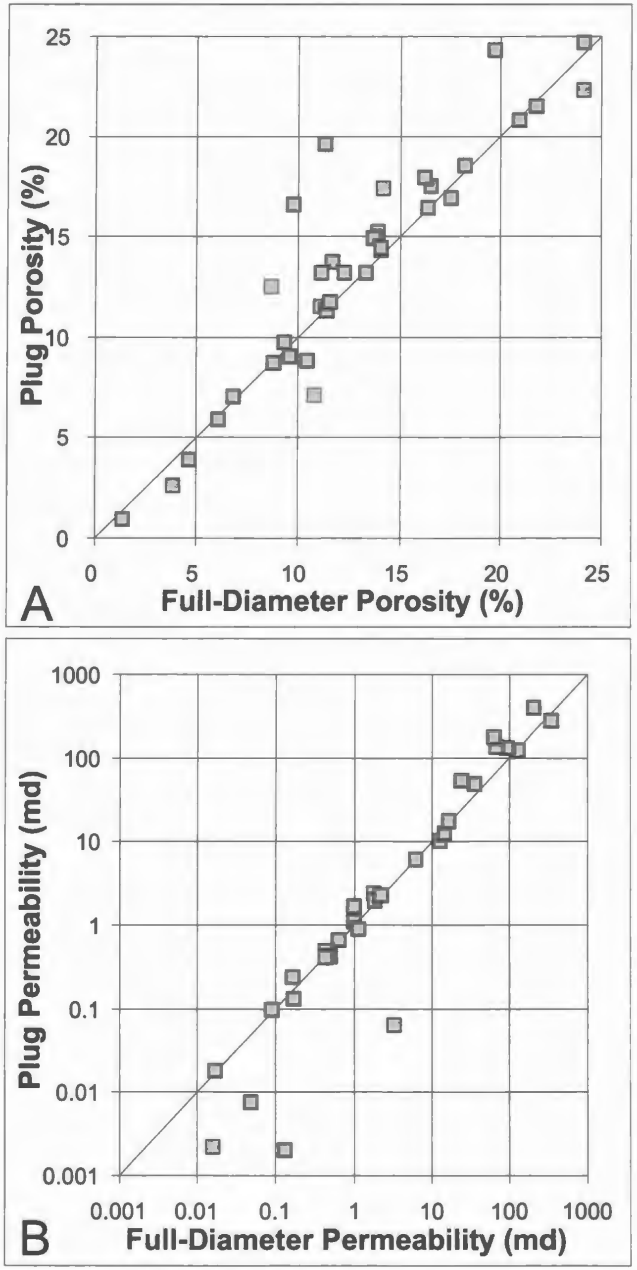

Crossplot of full-diameter core porosity versus plug porosity (A) and permeability (B) for samples in which the full-diameter cores did not exhibit any apparent microfracturing. Good correlation indicates that matrix-scale properties apply to full-diameter scale. Variance can be attributed to full-diameter core sampling multiple lithofaceis or a range in porosity not sampled by the corresponding core plug.

Figure 3.2.2

Crossplot of calculated interval drill stem test (DST) formation permeability versus average interval permeability calculated from full-diameter core for four wells and from core plugs in well 1. Routine core data were corrected for confining stress, Klinkenberg, and relative permeability effects so as to correspond to reservoir-condition values. Good correlation down to ~0.5 md shows matrix-scale control of flow in the region of DST investigation. Below 0.5 md microfractures in full-diameter core result in permeabilities higher than in the unfractured reservoir. Higher DST than core plug permeabilities can be interpreted to indicate that formation is not fractured in the range of investigation and that plug sampling density was probably not adequate to properly sample lower range of permeability.

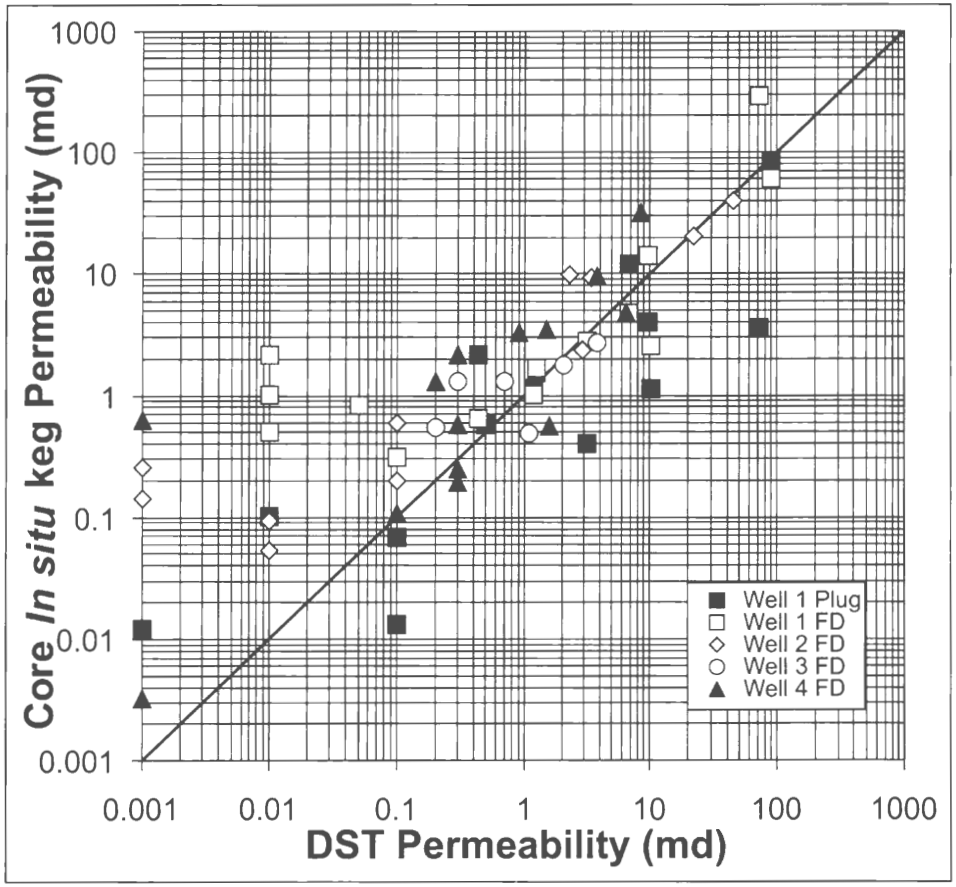

Figure 3.2.3

Layer	Formation	Upscaled K, md	DST K, md	Multiplier
1	Hrngtn-Paddock	5.668	6.9	1
2	Krider	47.422	90.30	1.9
3	Odell	0.017	9.7*	1
	Wnf SS			
4	Wnf LS	1.620	7.60	4.7
5	Gage	0.064	Not Tested	1.0
6	Towanda	1.666	1.20	1.0
7	B/TWND	1.859	Not Tested	1.0
8	FTRLY	0.948	0.43	1.0
9	L/FTRLY	0.019	0.001	1.0
10	B/FTRLY	0.039	0.1	1.0
11	WREFORD	0.107	0.5	4.7
12	A1_SH	0.001	Not Tested	1.0
13	A1_LM	0.023	3.141**	1.0
14	B1_SH	0.002	Not Tested	1.0
15	B1_LM	0.123	0.1	1.0
16	B2_SH	0.004	Not Tested	1.0
17	B2_LM	0.755	10.2	13.5
18	B3_SH	0.002	Not Tested	1.0
19	B3_LM	0.047	0.01	1.0
20	B4_SH	0.001	Not Tested	1.0
21	B4_LM	0.676	3.2	4.7
22	B5_SH	0.002	Not Tested	1.0
23	B5_LM	11.558	72.1	6.2
24	C_SH	0.002	Not Tested	1
25	C_LM	0.089	Not Tested	1
		* Not representative		
		** Not a very representative value		
		May not need a multiplier		

Table 3.2.1

	Name	1st Prod	Sim Name	Simulator start	Cum gas, mcf	Pr record date	First SI, psi
1	**Fulk1**	1/31/1951	PFulk	1/1/1951	12,880,765	1/01/1951	394
2	**Betts1**	7/31/1951	PBet	7/1/1951	10,271,314	6/30/1951	361
3	**Musgrove1**	11/30/1950	PMus	11/1/1950	12,519,815	10/31/1950	383
4	**Coxxon1**	12/31/1949	PCox	12/1/1949	12,481,346	11/30/1949	374
5	**Persinger1**	10/31/1953	PPer	10/1/1953	5,888,797	10/31/1955	372
6	**Trotter1-24**	7/31/1950	PTrot24	7/1/1950	6,140,333	6/30/1950	395
7	**Trotter1-25**	1/31/1950	PTrot25	1/1/1950	9,056,970	12/31/1949	385
8	**Vresland1**	7/31/1949	PVre	7/1/1949	16,244,041	12/31/1949	373
9	**Zimmerman1**	1/31/1938	PZim	1/1/1938	12,811,895	12/31/1937	422
				Total prod, bcf	98.3		

Table 3.3.1

Sp gr of gas	0.715 (Air = 1)	Ppc	662 psia	
Assume WHSP	422 psi	Tpc	380 R	
Well depth	3000 ft			
		Tbg head static temp	60 F	520 R
Est BHSP - Ist Pws	**453.7 psi**	Bottom hole static temp	90 F	550 R

Ist Iteration

Avg wellbore pr	437.8 psi
Avg wellbore temp	535 R
Ppr	0.66
Tpr	1.41
Z	0.925
s	0.162541
2nd Pws =	**457.7 psi**

2nd Iteration

Avg wellbore pr	439.9 psi
Ppr	0.66
Tpr	1.41
Z	0.925 **(within the limits of readability of the chart - Fig 3.7, page 112)**
s	remains same
Thus, Pws (BHSP) =	**458 psi**

Table 3.3.2

History match - Chase Parent wells

RUN 1 – **Pi = 460 psi., ff = 2 for PTrot24 & ff = 6 for all other Chase Parent wells.**

CH wells fractures constrained within Chase and CG wells in CG. CH fractures initiated – Jan 1, 1960.

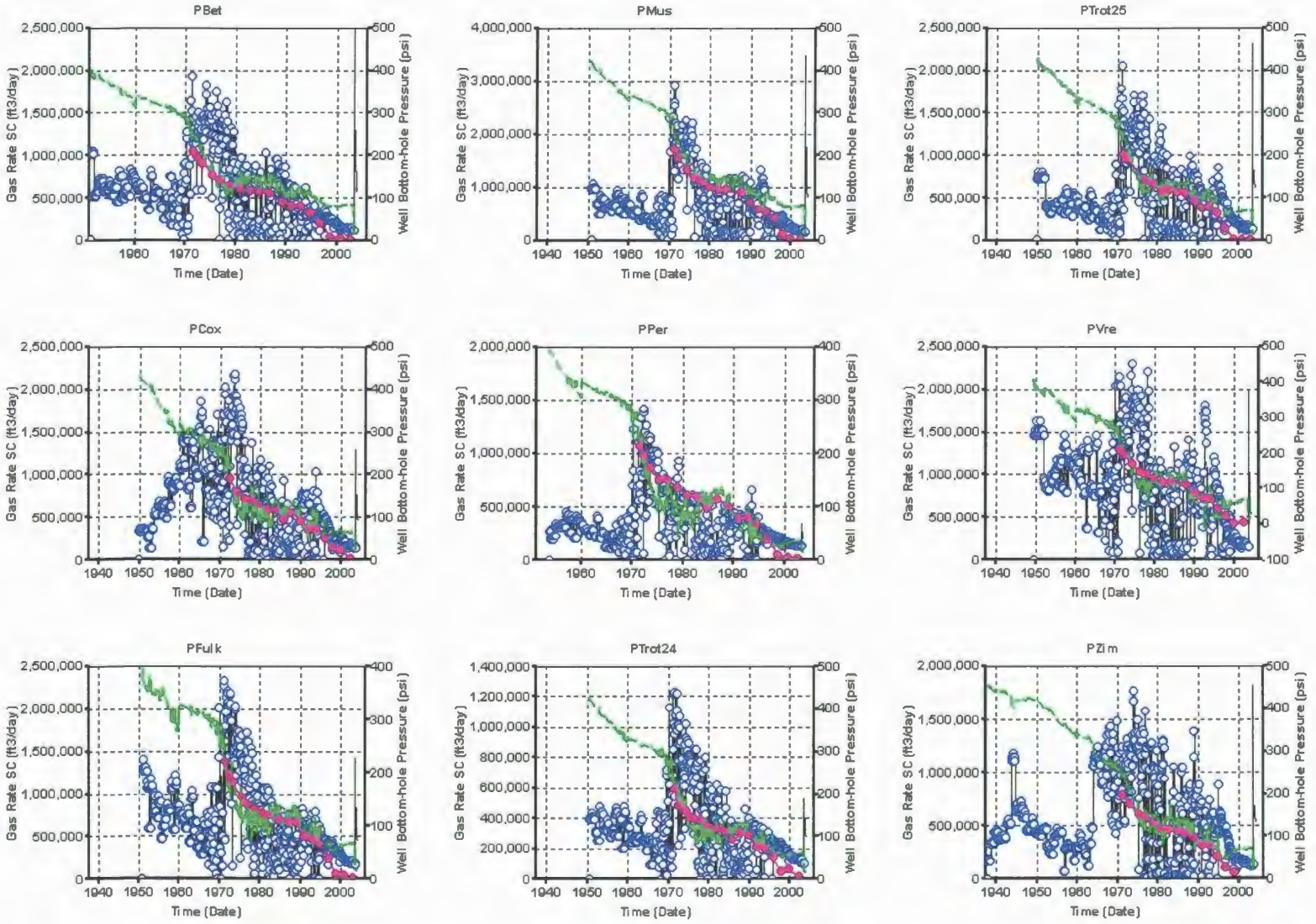

Black thin line – Simulator (Sim) calculated gas rate, Blue circles – historic gas production rate, Green broken line – Sim bottom hole pressure (BHP flowing), Magenta circles – Well head flowing pressure (WHFP).

Figure 4.1.1

RUN 1 – Pi = 460 psi., ff = 6 for for all Chase Infill (CH I) wells

His Match of CH I wells

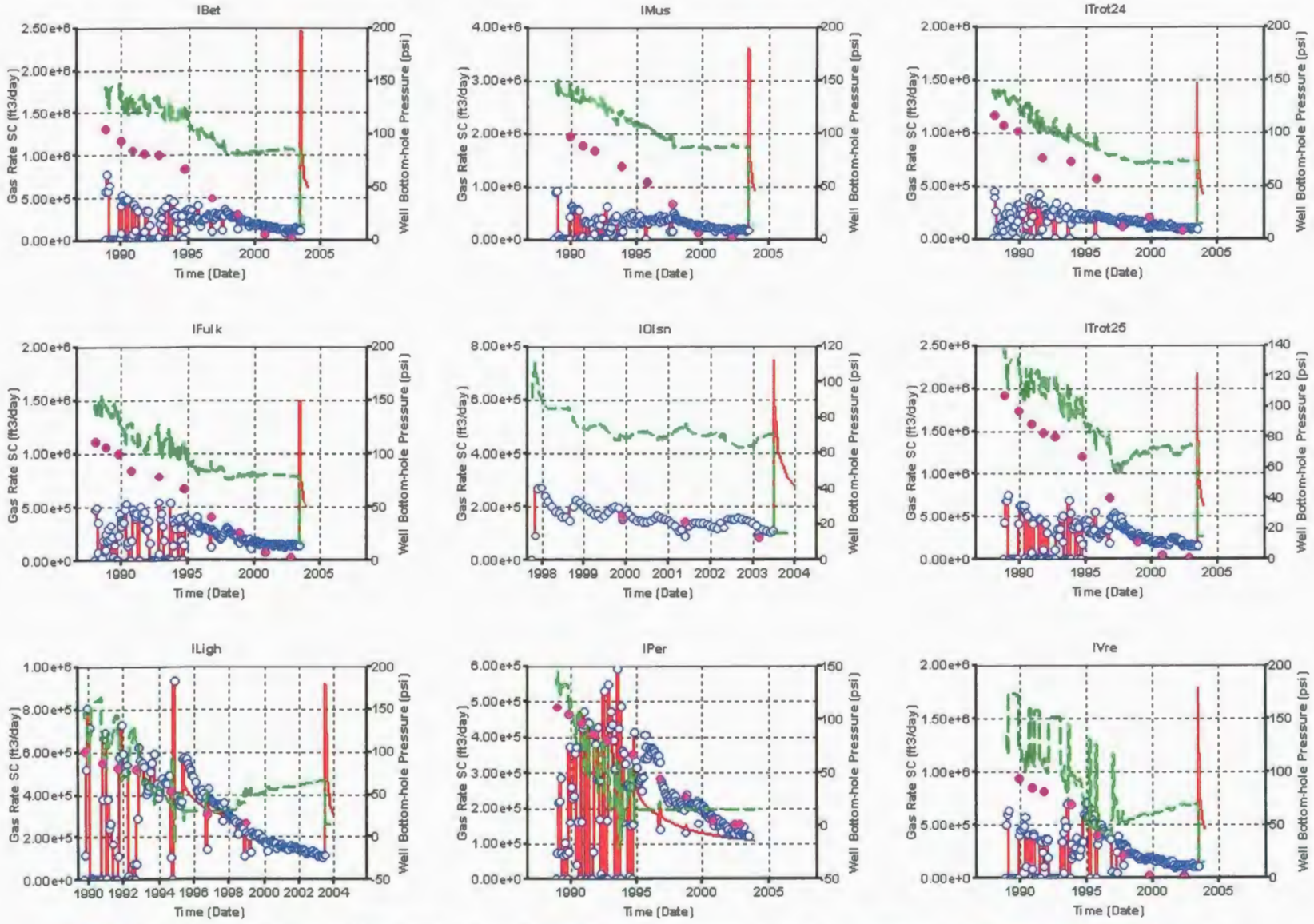

Red line – Simulator (Sim) calculated gas rate, Blue circles – historic gas production rate, Green broken line – Sim bottom hole pressure (BHP flowing), Magenta circles – Well head flowing pressure (WHFP).

Figure 4.1.2

RUN 1 – Pi = 460 psi., ff = 6 for for all wells

His Match of CG wells

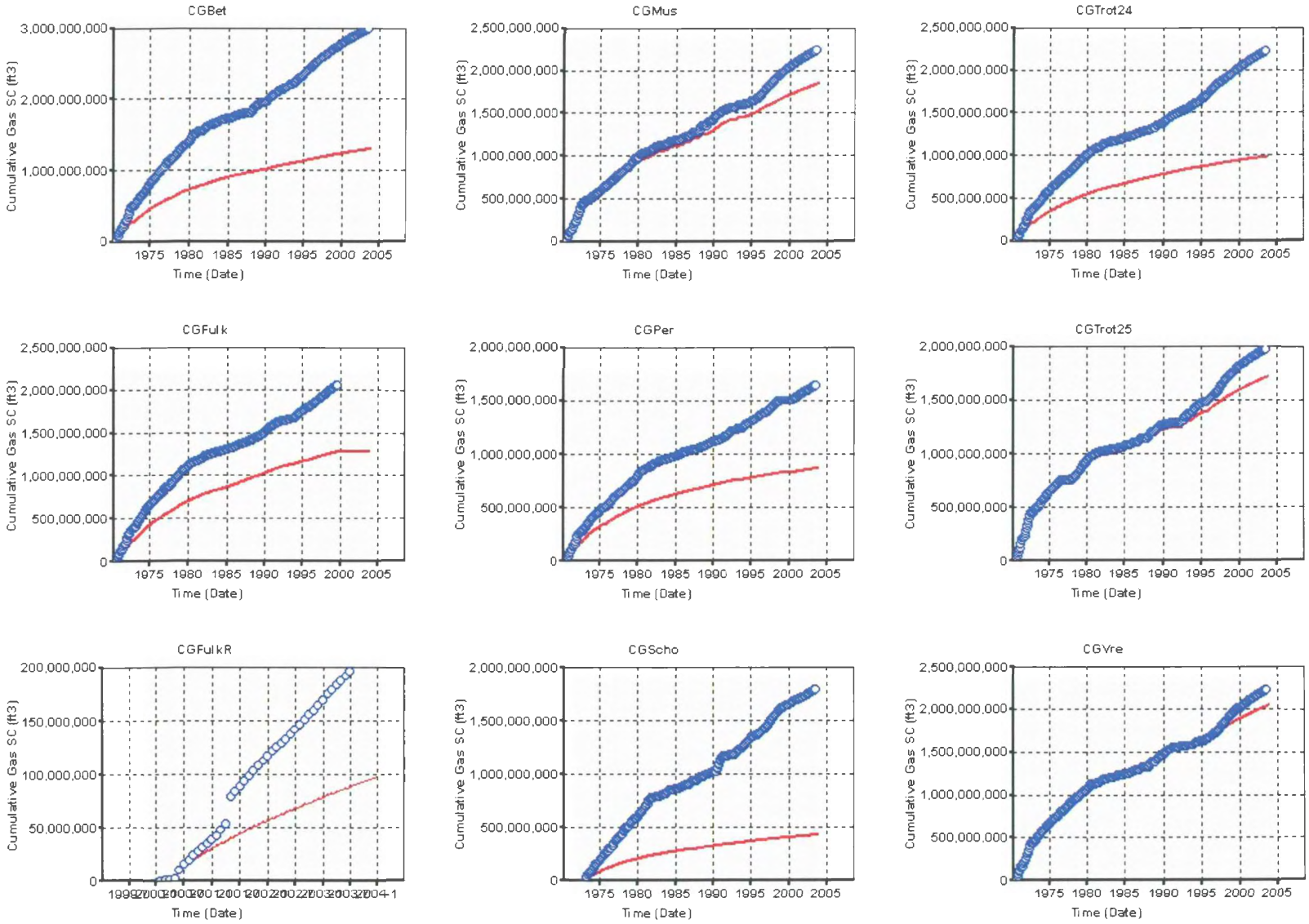

Red line – Simulator (Sim) calculated cumulative gas prod, **Blue** circles – historic cumulative gas production

Figure 4.1.3

Pr distribution as of Jan 1970 – just before CG wells came online

RUN 1 – K adj. Pi = 460 psi.

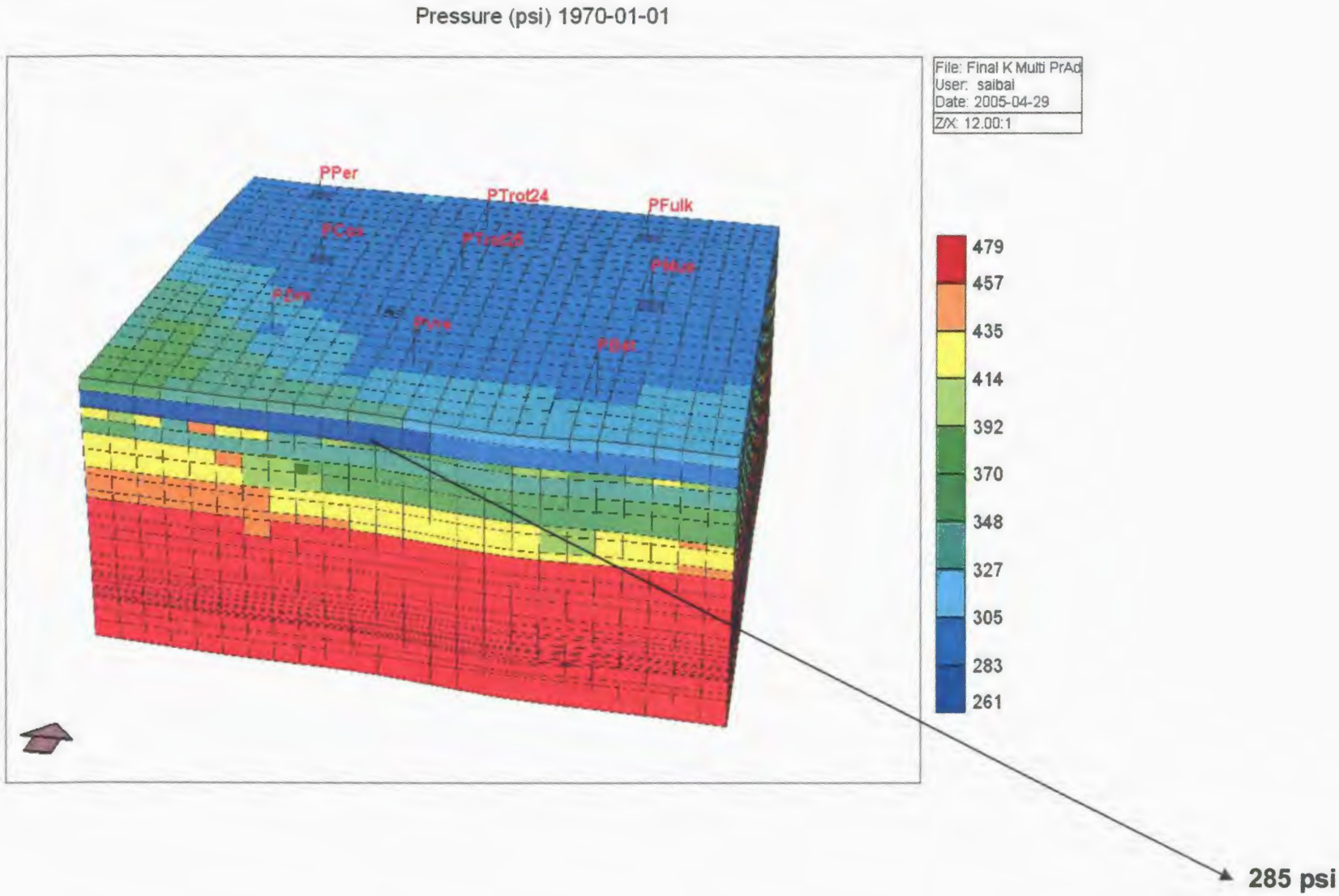

Figure 4.1.4

2nd run – Pi = 460 psi.,
ff = 2 for PTrot24 & ff = 6 for all other CH P wells

CH P history matches (cum prod) when CG Fractures extended to L2

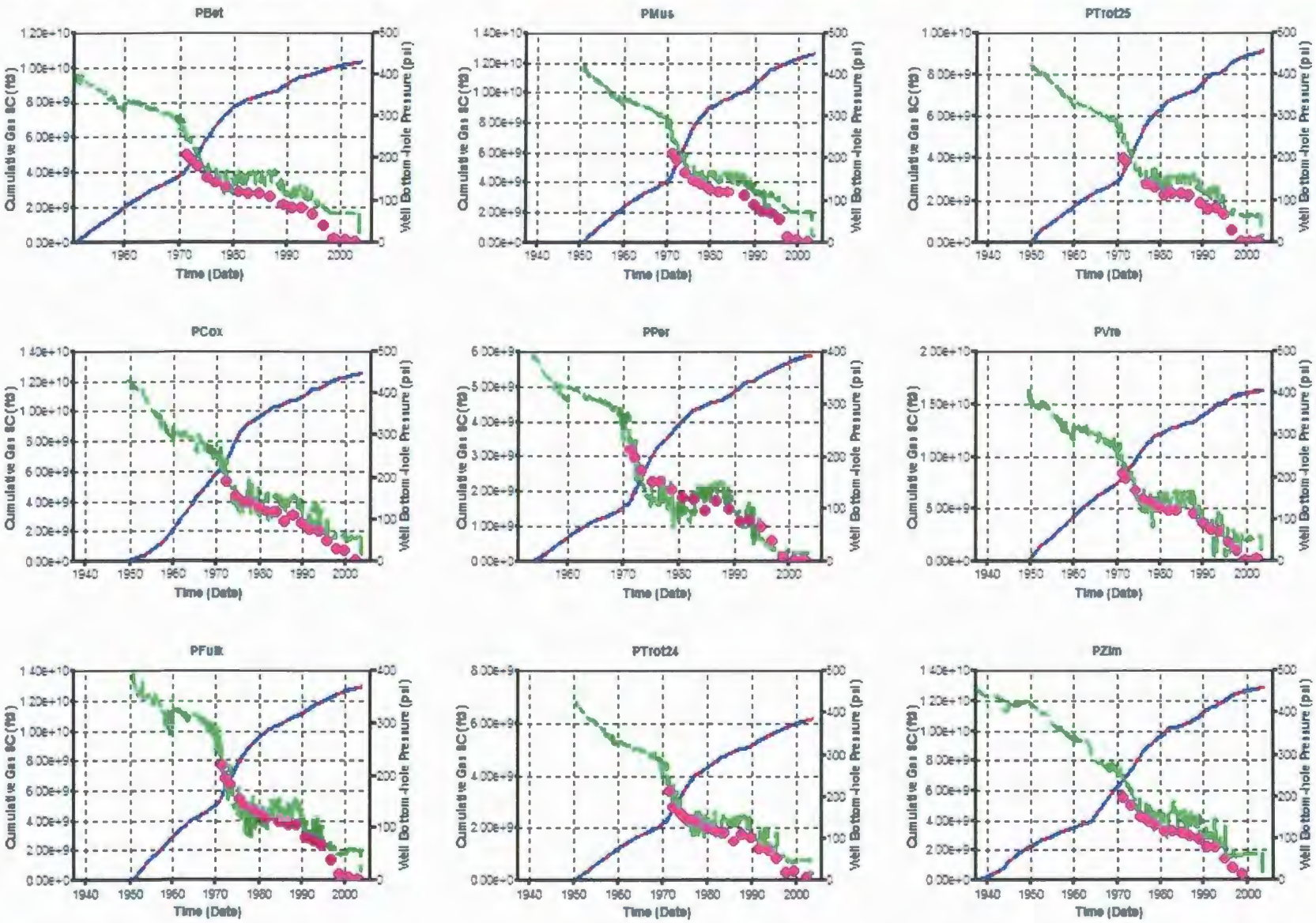

Red line – Simulator (Sim) calculated cumulative gas, Blue broken line – historic cumulative gas production, Green broken line – Sim bottom hole pressure (BHP flowing), Magenta circles – Well head flowing pressure (WHFP).

Figure 4.2.1

CH P history matches (prod rate) when CG Fractures extended to L2

2nd run – Pi = 460 psi.,
ff = 2 for PTrot24 & ff = 6 for all others CH P wells

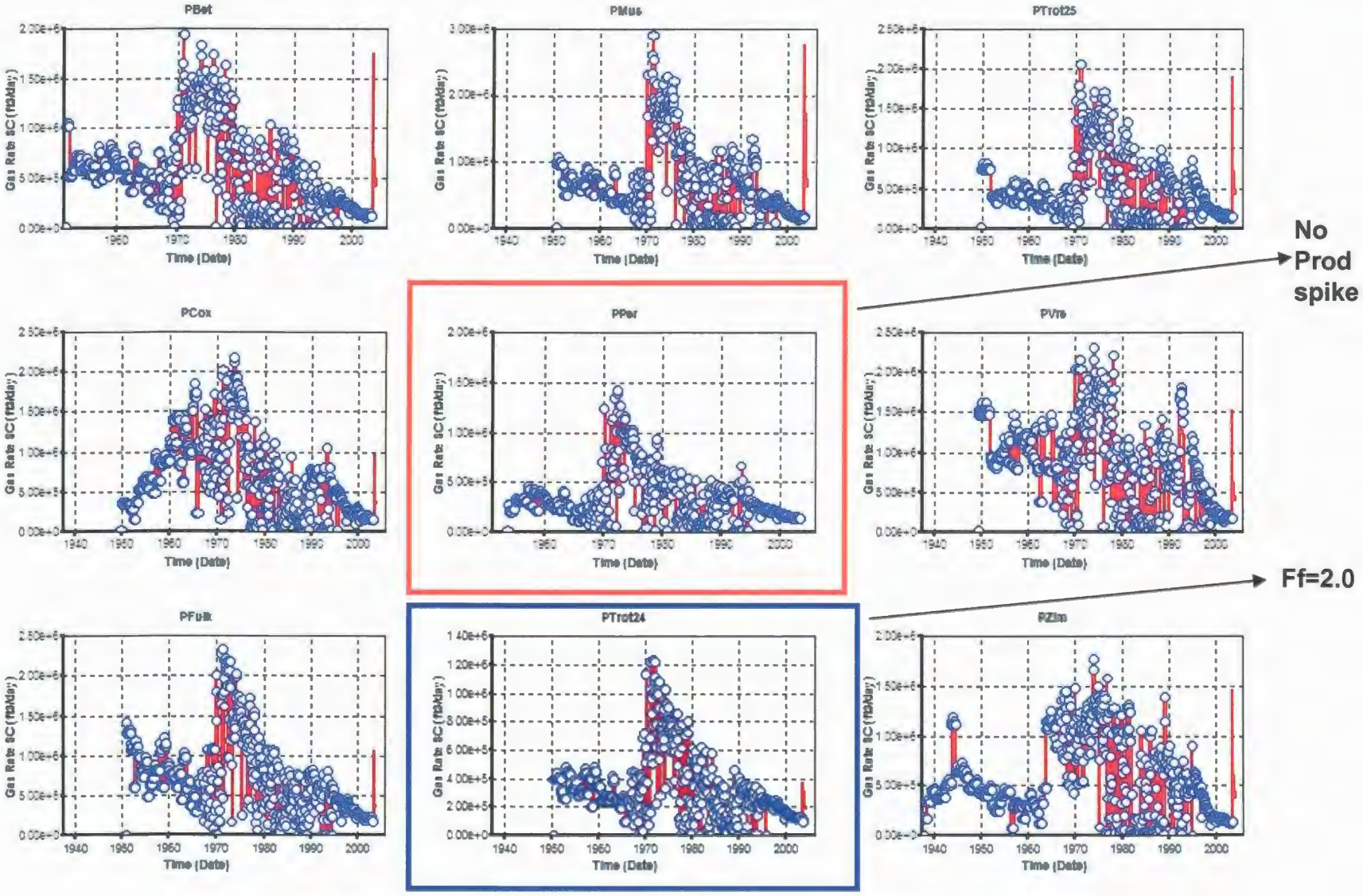

Red line – Simulator (Sim) calculated gas rate, **Blue** circles – historic gas production rate,

Figure 4.2.2

2nd run – Pi = 460 psi.,
ff = 6 for all CH I wells

CH I history matches (Cum prod) when CG Fractures extended to L2

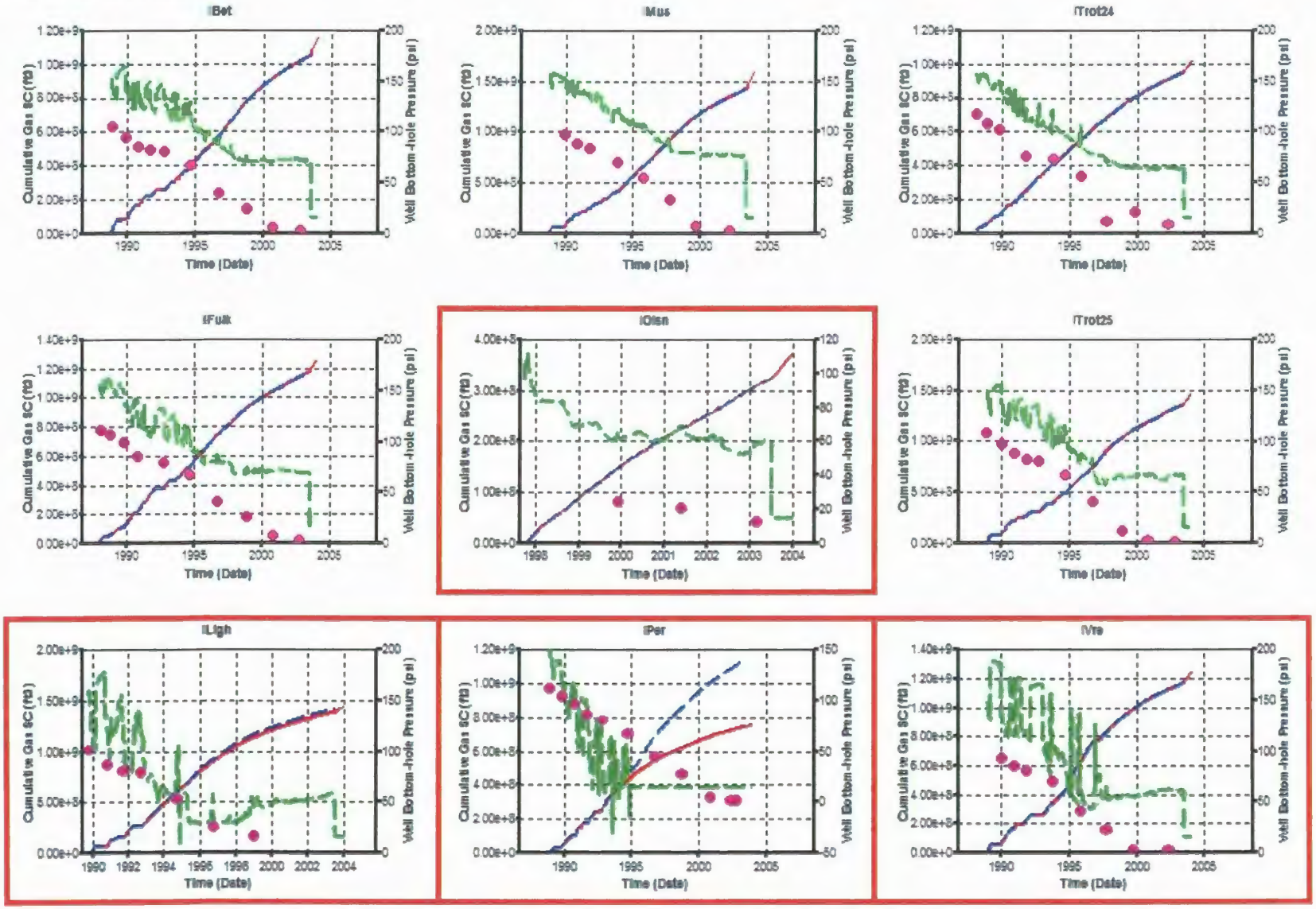

Red line – Simulator (Sim) calculated cum gas, Blue broken line – historic cum gas production, Green broken line – Sim bottom hole pressure (BHP flowing), Magenta circles – Well head flowing pressure (WHFP).

Border well.

Figure 4.2.3

2nd run – K adj. Pi = 460 psi.
ff = 6 for all CG wells

CG history matches (Cum prod) when CG Fractures extended to L2

CGFulkR is a border well that is replacement of CGFulk.

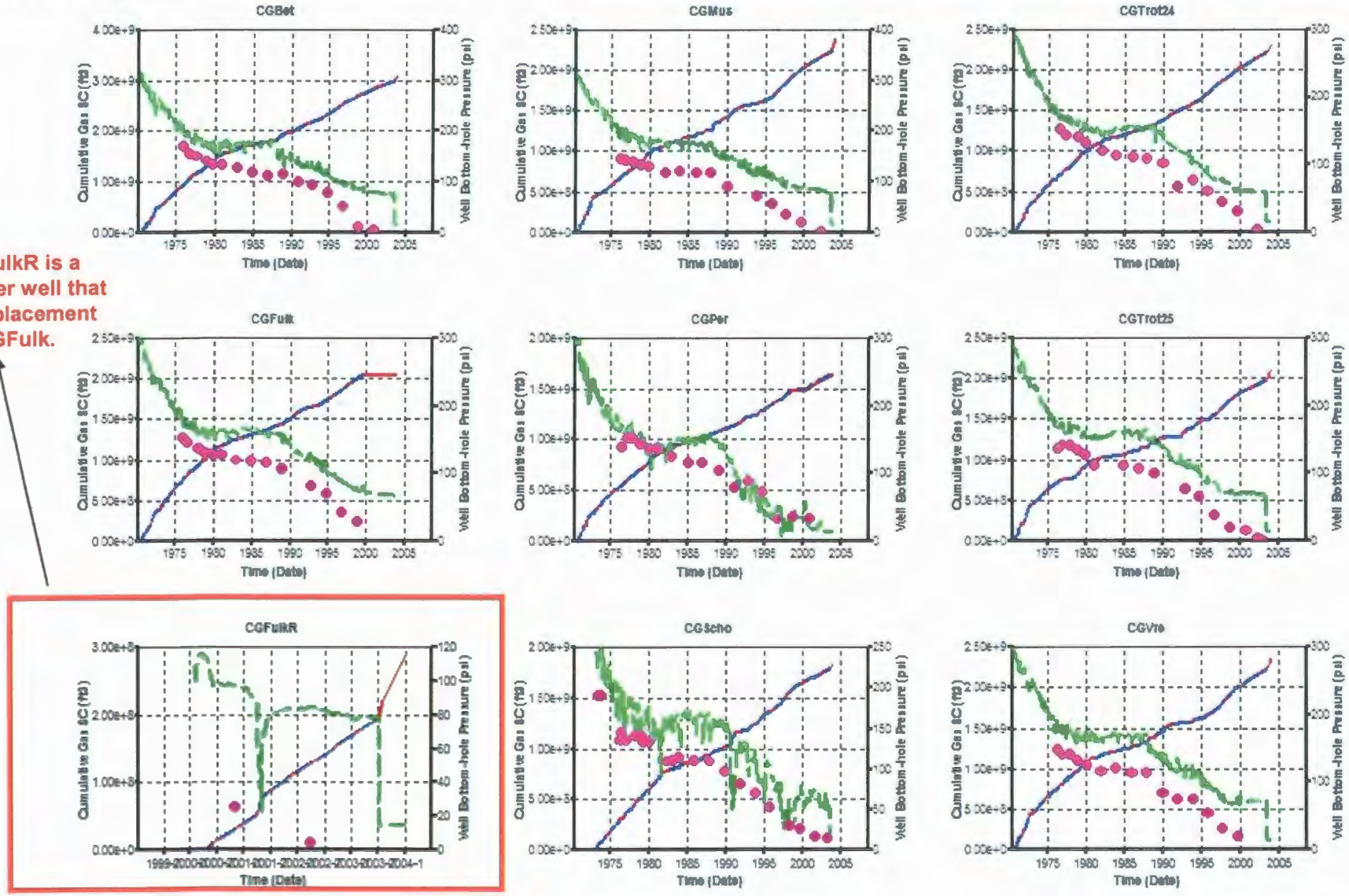

Red line – Simulator (Sim) calculated cum gas, Blue broken line – historic cum gas production, Green broken line – Sim bottom hole pressure (BHP flowing), Magenta circles – Well head flowing pressure (WHFP).

Figure 4.2.4a

2nd run – K adj. Pi = 460 psi.
ff = 6 for all CG wells

CG history matches (Cum prod) when CG Fractures extended to L2

CGZim

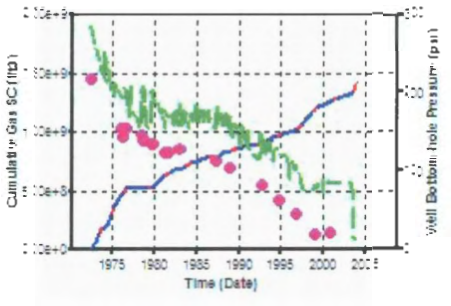

Red line – Simulator (Sim) calculated cum gas, Blue broken line – historic cum gas production, Green broken line -- Sim bottom hole pressure (BHP flowing), Magenta circles -- Well head flowing pressure (WHFP).

Figure 4.2.4b

3rd Run – Pi = 435 psi, OGIP = 185 bcf.

Ff adjusted for CH P wells (ff between 5 and 9).

CH P history matches when CG Fractures extend to L2 & Pi = 435 psi

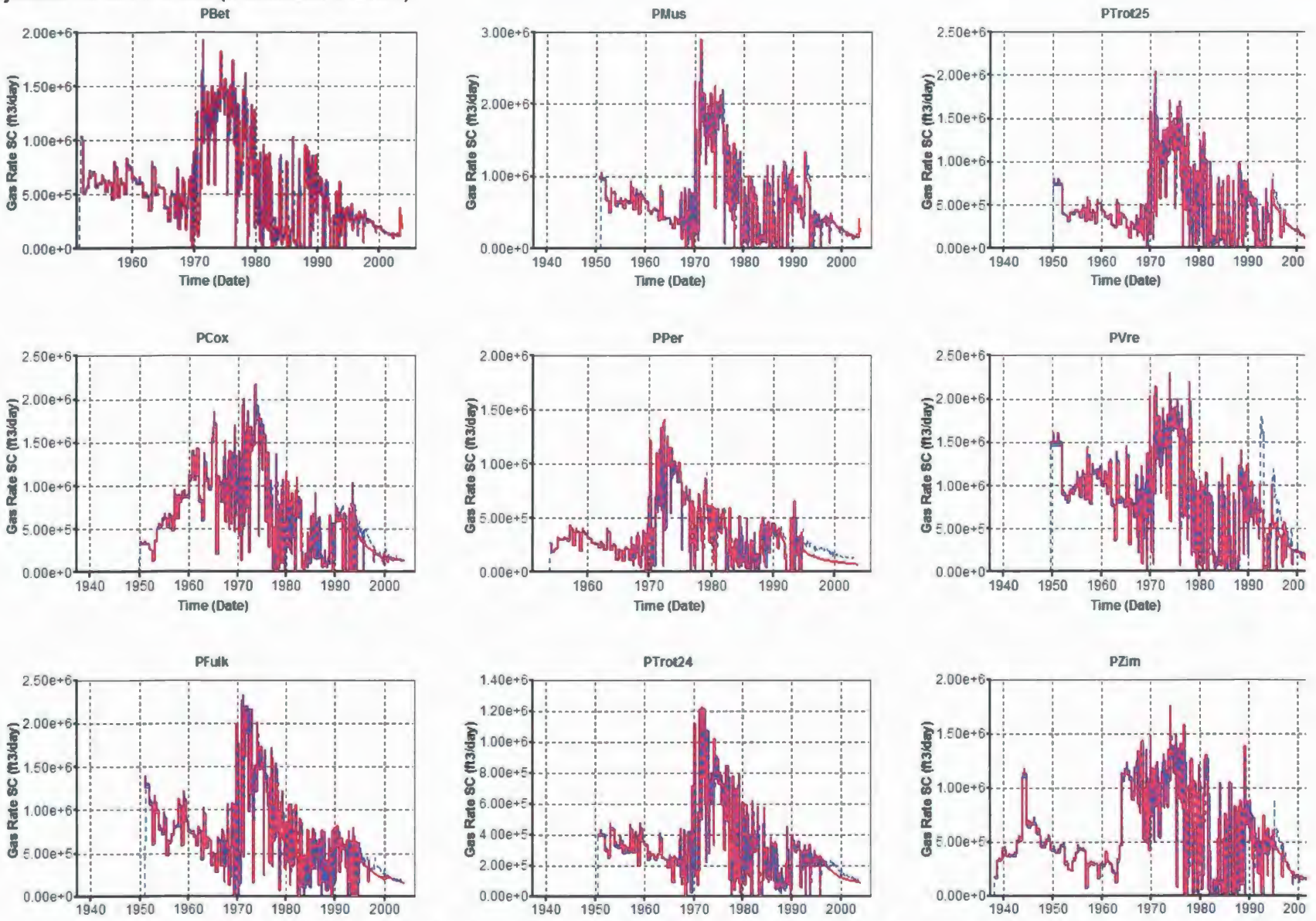

Red line – Simulator (Sim) calculated cum gas, Blue broken line – historic cum gas production

Figure 4.3.1

3rd Run – Pi = 435 psi, OGIP = 185 bcf.

Ff adjusted for CH P wells (ff between 5 and 9).

CH P flowing Pr matches when CG Fractures extend to L2 & Pi = 435 psi

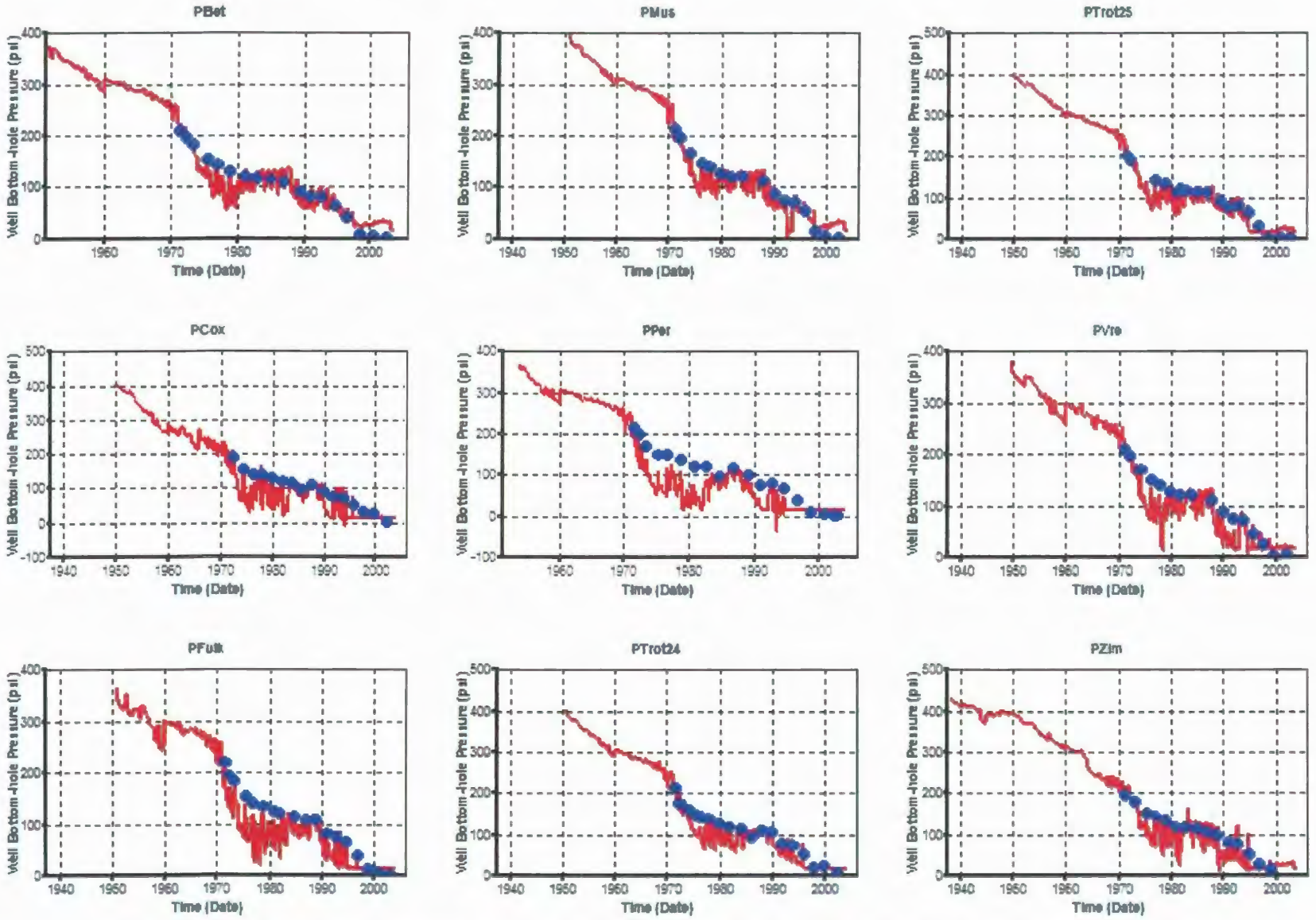

Red broken line – Sim bottom hole pressure (BHP flowing), Blue circles – Well head flowing pressure (WHFP).

Figure 4.3.2

3rd Run – Pi = 435 psi, OGIP = 185 bcf.

Ff for CG wells set at 6.

CG history matches when CG Fractures extend to L2 & Pi = 435 psi

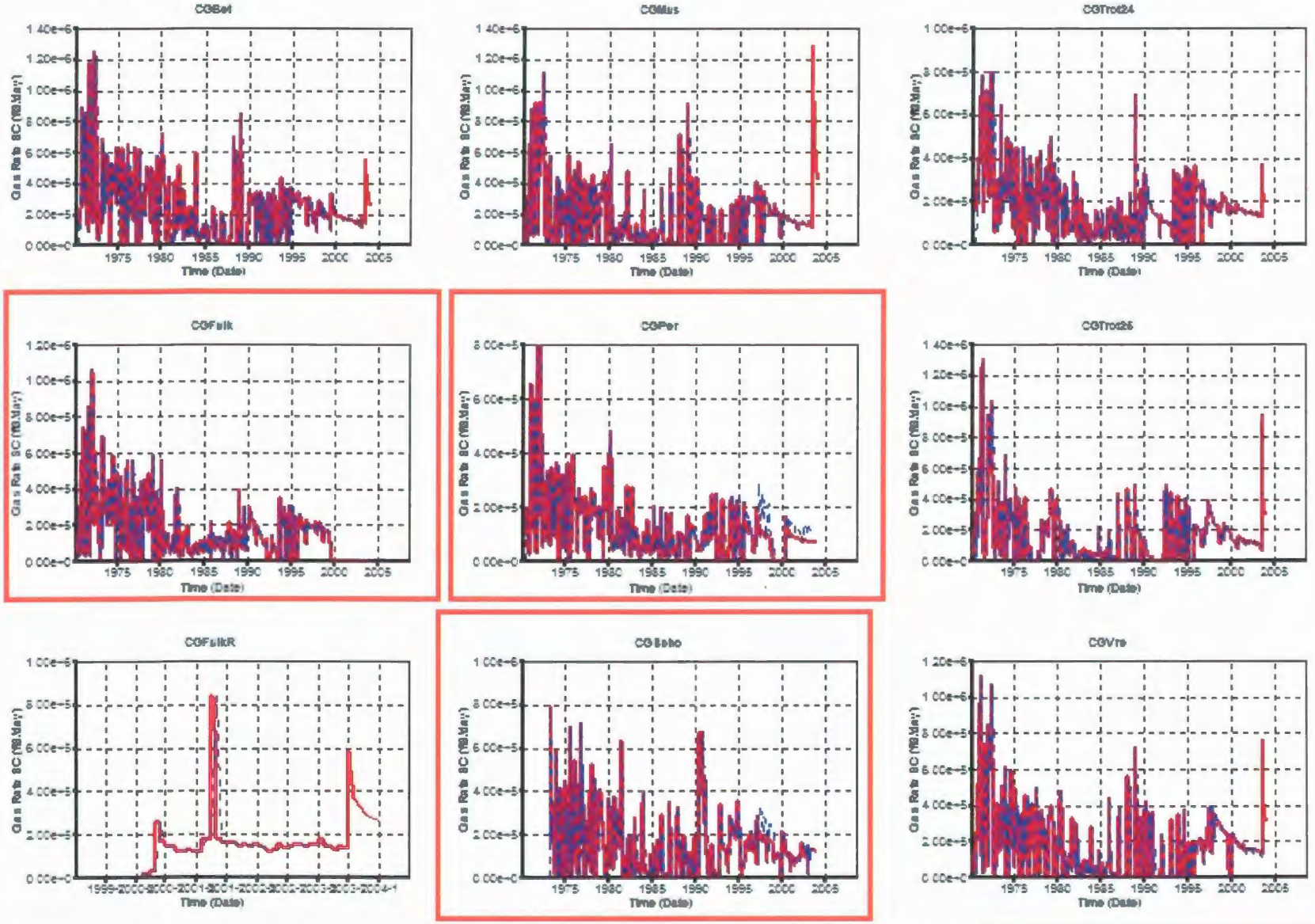

Red line – Simulator (Sim) calculated cum gas, Blue broken line – historic cum gas production. Wells without production spikes.

Figure 4.3.2a

3rd Run – Pi = 435 psi, OGIP = 185 bcf.

Ff for CG wells set at 6.

CG history matches when CG Fractures extend to L2 & Pi = 435 psi

CGZim

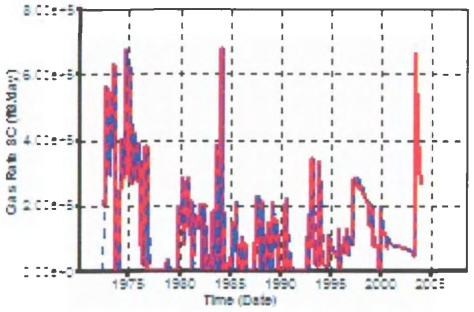

Red line – Simulator (Sim) calculated cum gas, Blue broken line – historic cum gas production

Figure 4.3.3b

4th Run – Pi = 435 psi, OGIP = 185 bcf.

Ff for CG wells adjusted selectively.

CG history matches when CG Fractures extend to L2 & Pi = 435 psi

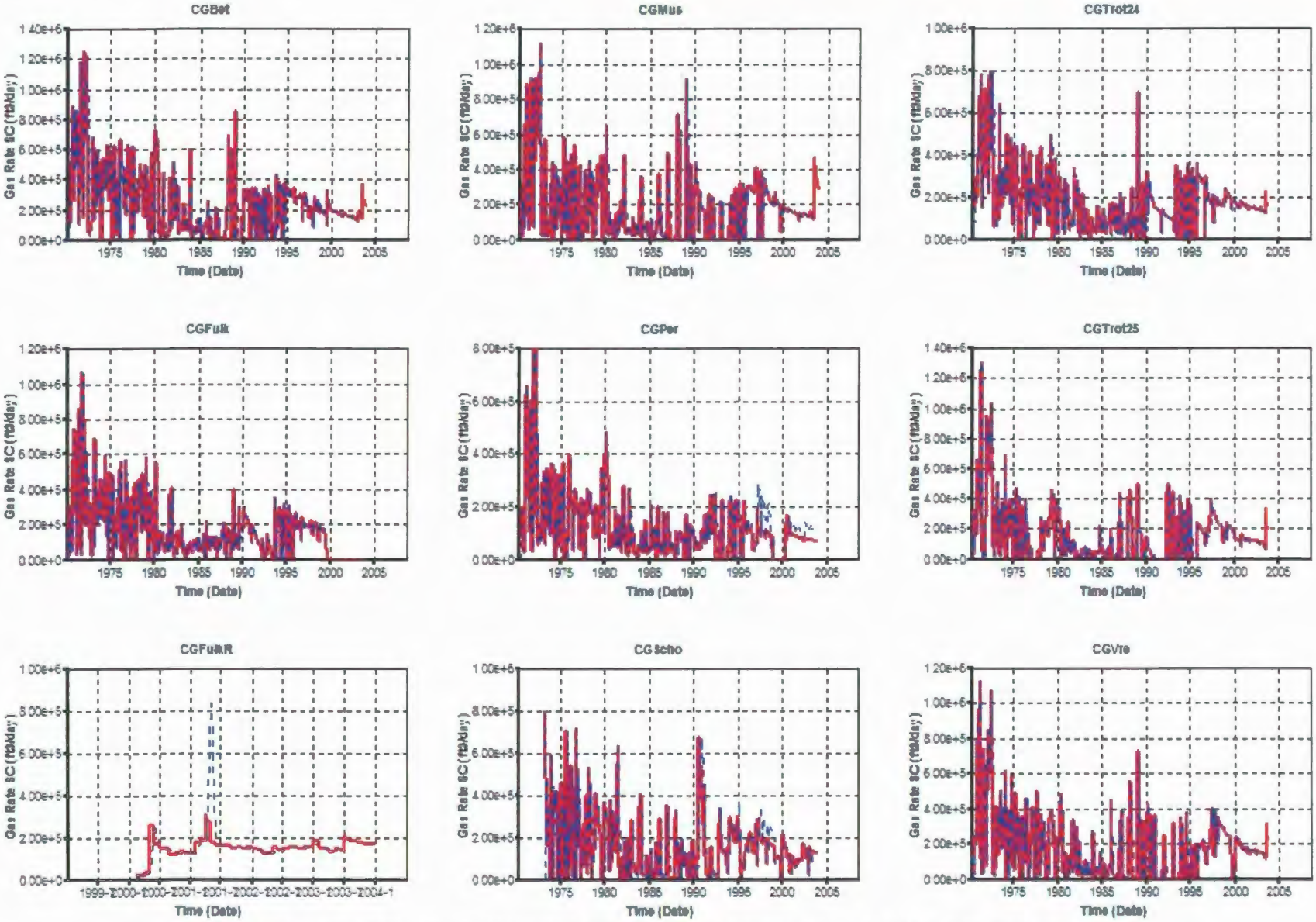

Red line – Simulator (Sim) calculated cum gas, Blue broken line – historic cum gas production

Figure 4.4.1a

4th Run – Pi = 435 psi, OGIP = 185 bcf.

Ff for CG wells adjusted selectively.

CG history matches when CG Fractures extend to L2 & Pi = 435 psi

CGZim

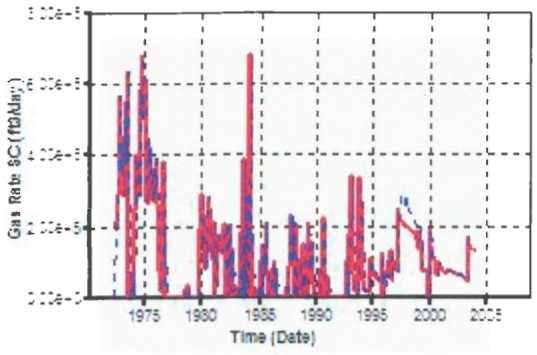

Red line – Simulator (Sim) calculated cum gas, Blue broken line – historic cum gas production

Figure 4.4.1b

5th Run – Pi = 423 psi, OGIP = 179.5 bcf.

Ff for CH P wells set at 6.

CH P history matches when CG Fractures extend to L2 & Pi = 423 psi

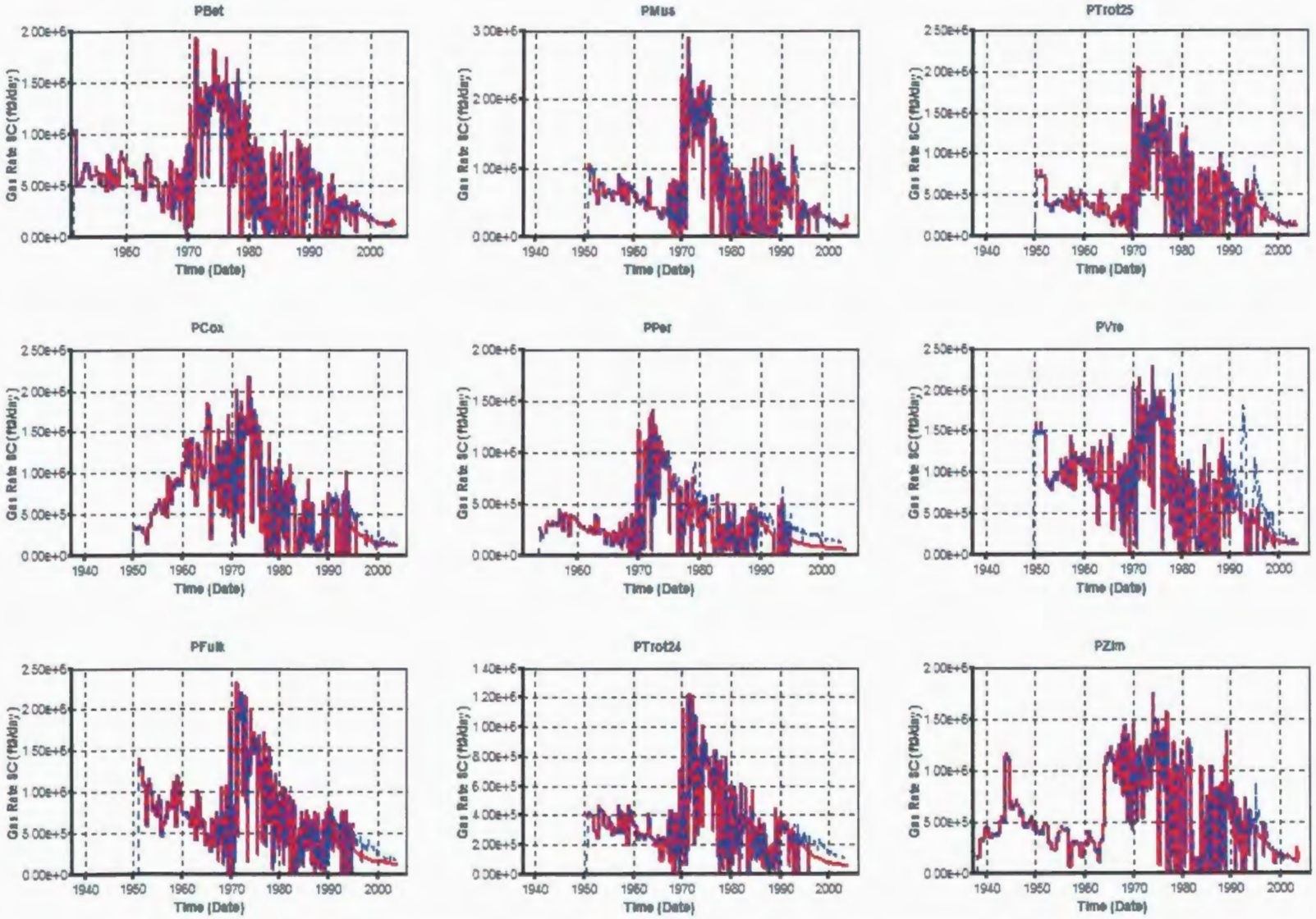

Red line – Simulator (Sim) calculated cum gas, Blue broken line – historic cum gas production

Figure 4.5.1

5th Run – Pi = 423 psi, OGIP = 179.5 bcf.

Ff for CG wells set at 6.

CG history matches when CG Fractures extend to L2 & Pi = 423 psi

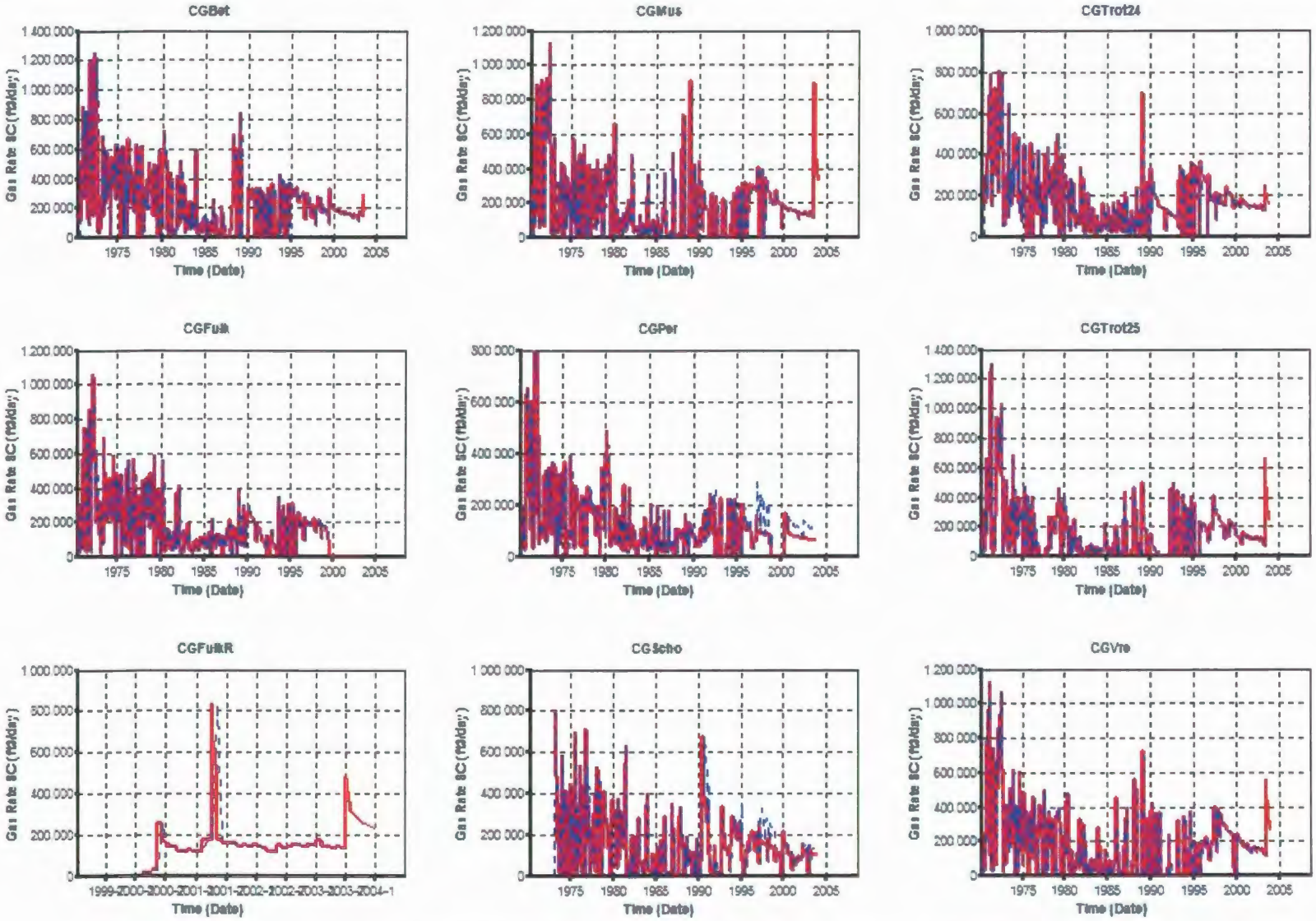

Red line – Simulator (Sim) calculated cum gas, Blue broken line – historic cum gas production

Figure 4.5.2a

5th Run – Pi = 423 psi, OGIP = 179.5 bcf.

Ff for CG wells set at 6.

CG history matches when CG Fractures extend to L2 & Pi = 423 psi

CGZim

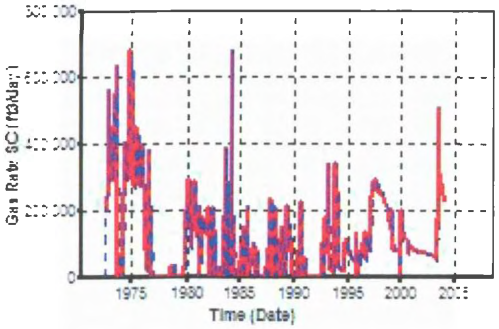

Red line – Simulator (Sim) calculated cum gas, Blue broken line – historic cum gas production

Figure 4.5.2b

CH P history matches when CG Fractures extend to L2 & Pi = 423 psi

6th Run – Pi = 423 psi, OGIP = 179.5 bcf.

Ff for CH P wells adjusted around 6 (between 5 and 9).

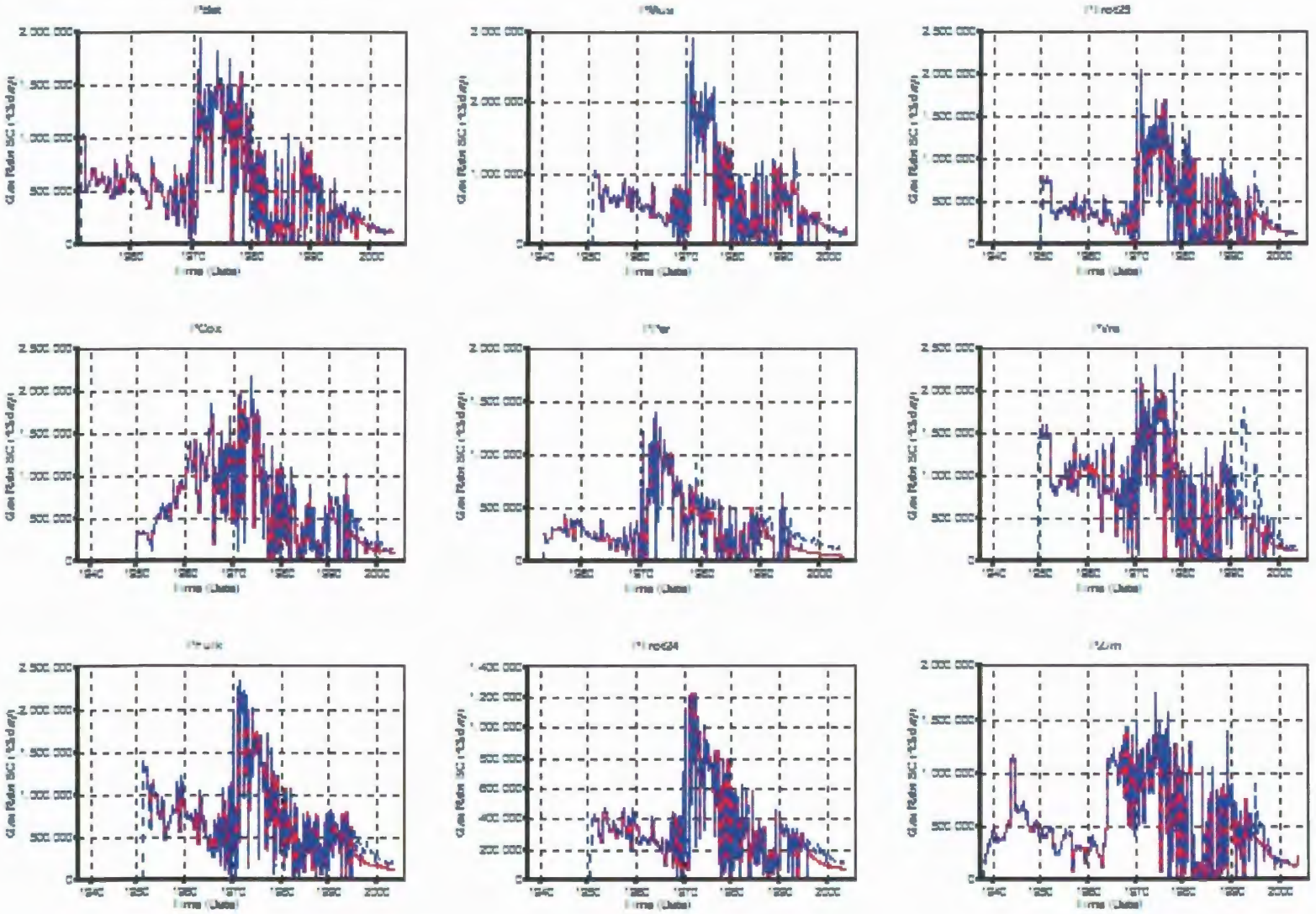

Red line – Simulator (Sim) calculated cum gas, Blue broken line – historic cum gas production

Figure 4.6.1

CH P flowing pr history matches when CG Fractures extend to L2 & Pi = 423 psi

6th Run – Pi = 423 psi, OGIP = 179.5 bcf.

Ff for CH P wells adjusted around 6 (between 5 and 9).

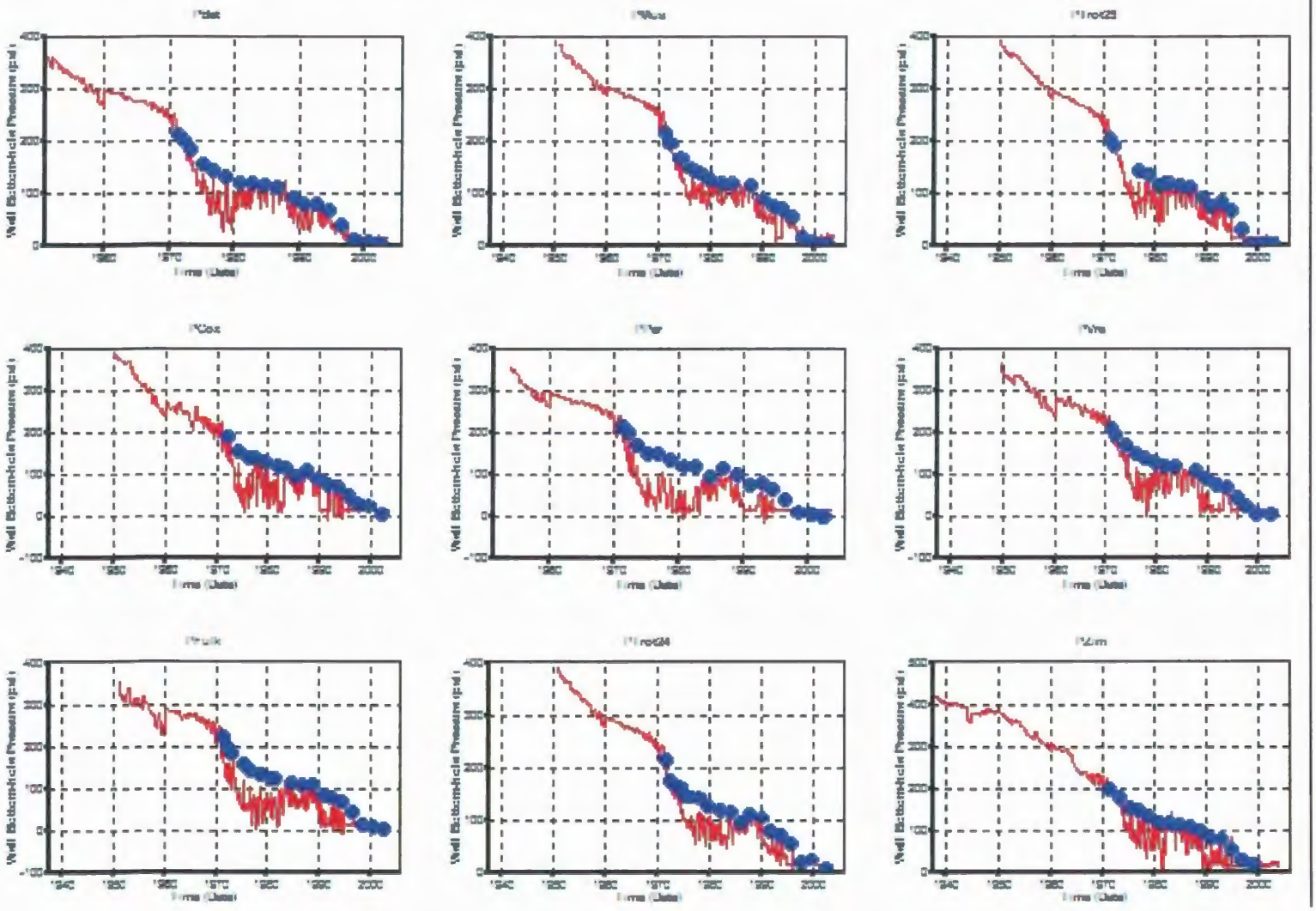

Red broken line – Sim bottom hole pressure (BHP flowing), Blue circles – Well head flowing pressure (WHFP).

Figure 4.6.2

CG history matches when CG Fractures extend to L2 & Pi = 423 psi

6th Run – Pi = 423 psi, OGIP = 179.5 bcf.

Ff for CG wells adjusted around 6 (between 5 and 9).

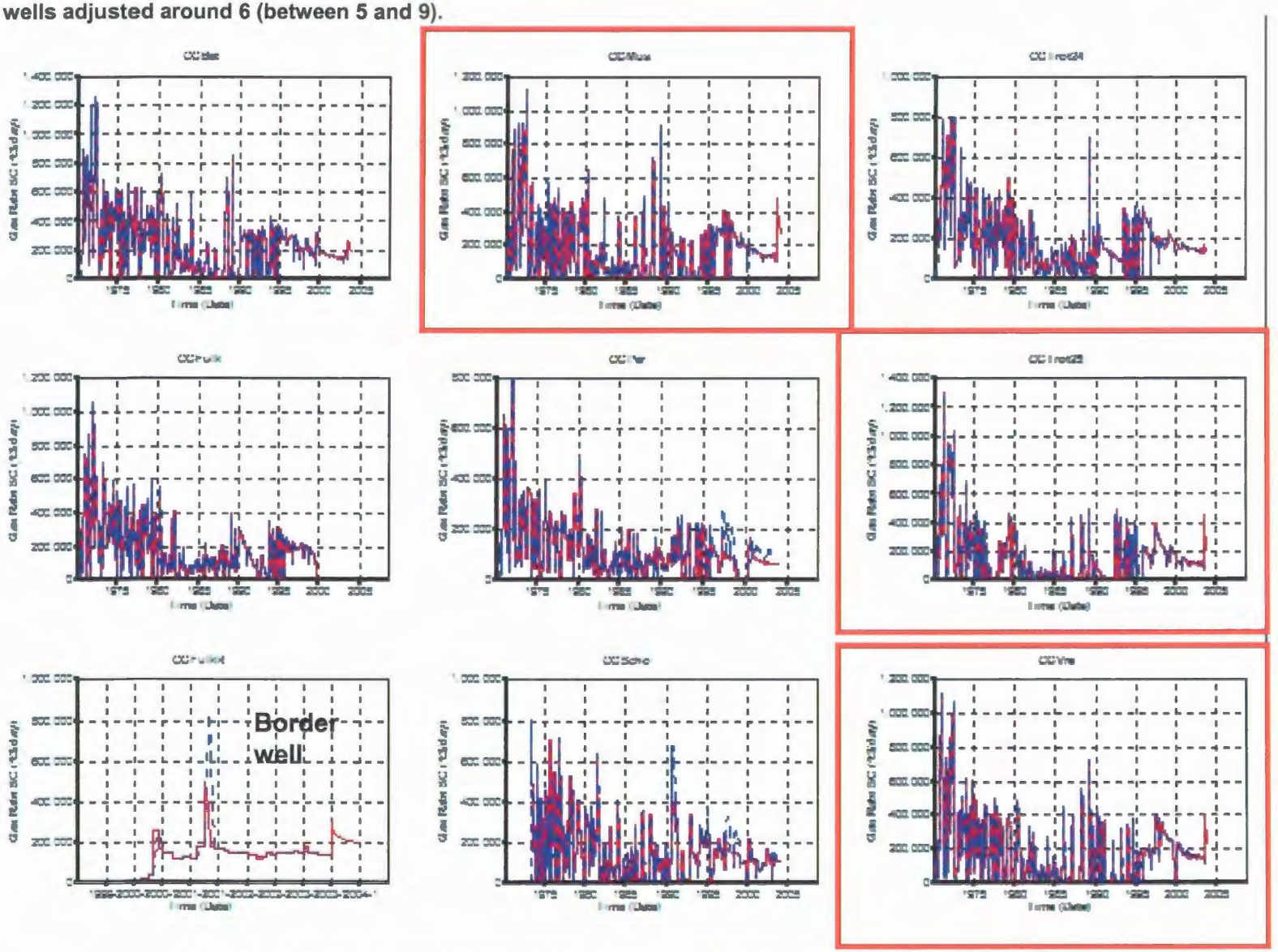

Red line – Simulator (Sim) calculated cum gas, Blue broken line – historic cum gas production

. Some wells still show a production spike.

Figure 4.6.3a

CG history matches when CG Fractures extend to L2 & Pi = 423 psi

6th Run – Pi = 423 psi, OGIP = 179.5 bcf.

Ff for CG wells adjusted around 6 (between 5 and 9).

CGZim

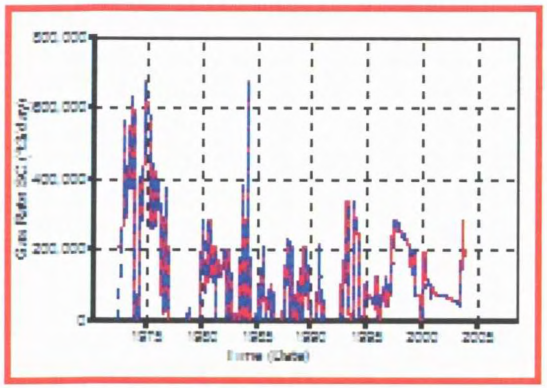

Red line – Simulator (Sim) calculated cum gas, Blue broken line – historic cum gas production

Some wells still show a production spike.

Figure 4.6.3b

CG flowing pr history matches when CG Fractures extend to L2 & Pi = 423 psi

6th Run – Pi = 423 psi, OGIP = 179.5 bcf.

Ff for CG wells adjusted around 6 (between 5 and 9).

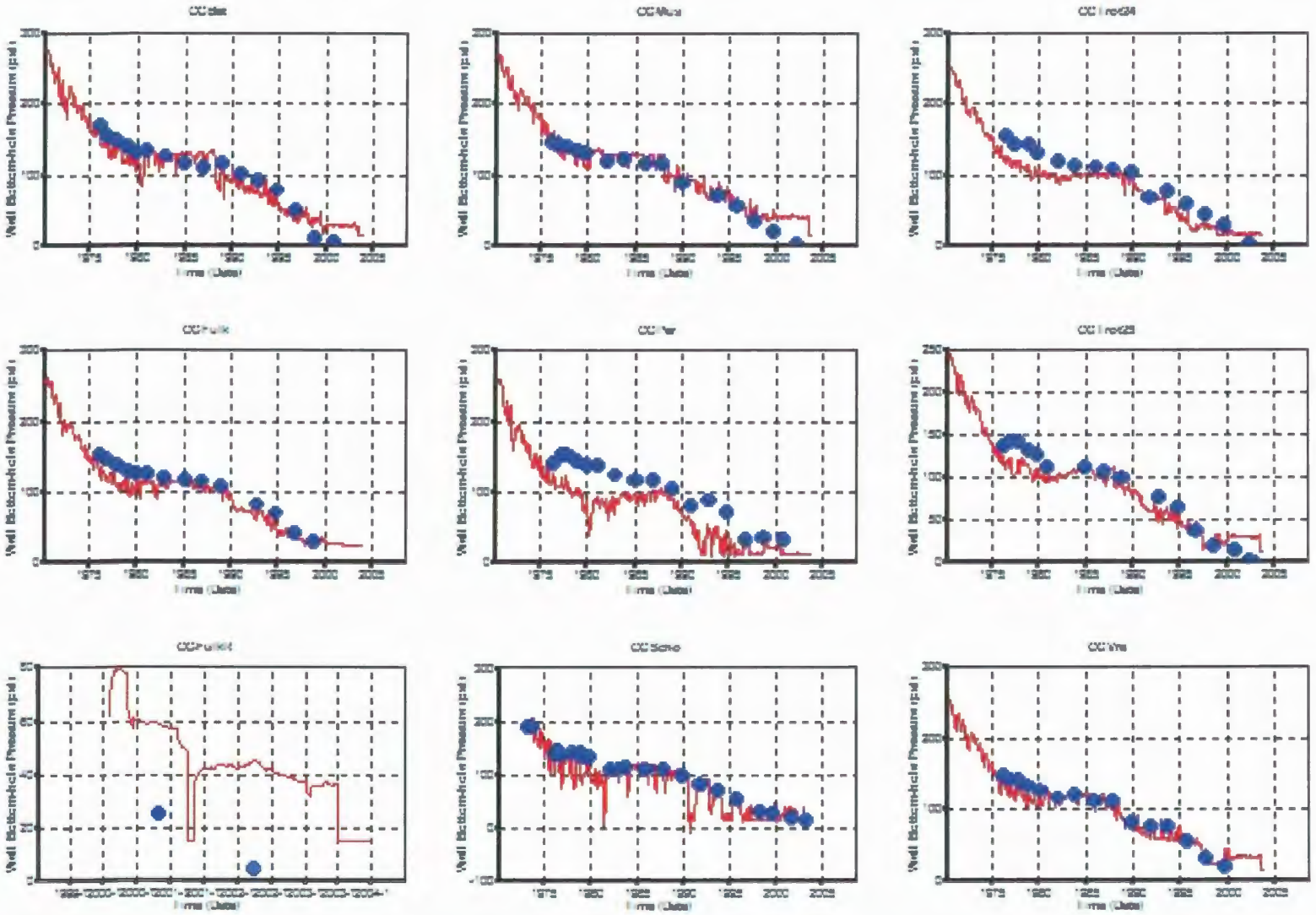

Red broken line – Sim bottom hole pressure (BHP flowing), Blue circles – Well head flowing pressure (WHFP).

Figure 4.6.4a

CG history matches when CG Fractures extend to L2 & Pi = 423 psi

6th Run – Pi = 423 psi, OGIP = 179.5 bcf.

Ff for CG wells adjusted around 6 (between 5 and 9).

CGZim

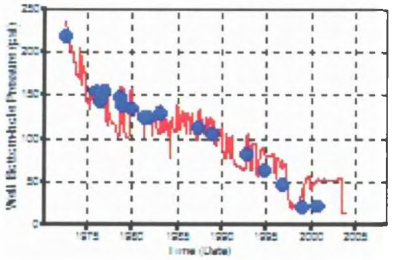

Red broken line – Sim bottom hole pressure (BHP flowing), Blue circles – Well head flowing pressure (WHFP).

Figure 4.6.4b

CH I history matches when CG Fractures extend to L2 & Pi = 423 psi

6th Run – Pi = 423 psi, OGIP = 179.5 bcf.

Ff for CH I wells adjusted around 6 (between 5 and 9).

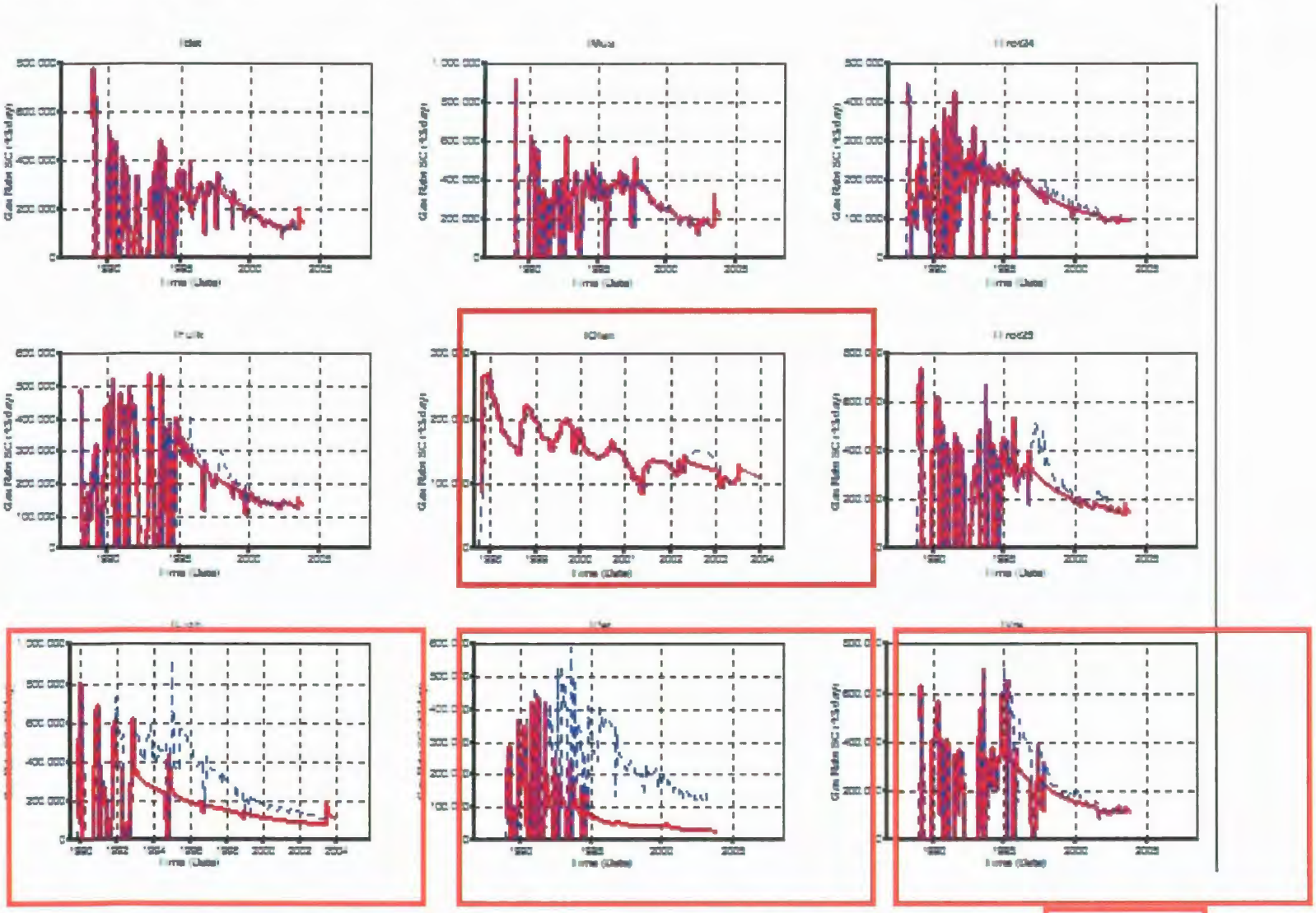

Red line – Simulator (Sim) calculated gas rate, Blue broken line – historic gas rate. Border wells.

Figure 4.6.5

CH I flowing pressure history matches when CG Fractures extend to L2 & Pi = 423 psi

6th Run – Pi = 423 psi, OGIP = 179.5 bcf.

Ff for CH I wells adjusted around 6 (between 5 and 9).

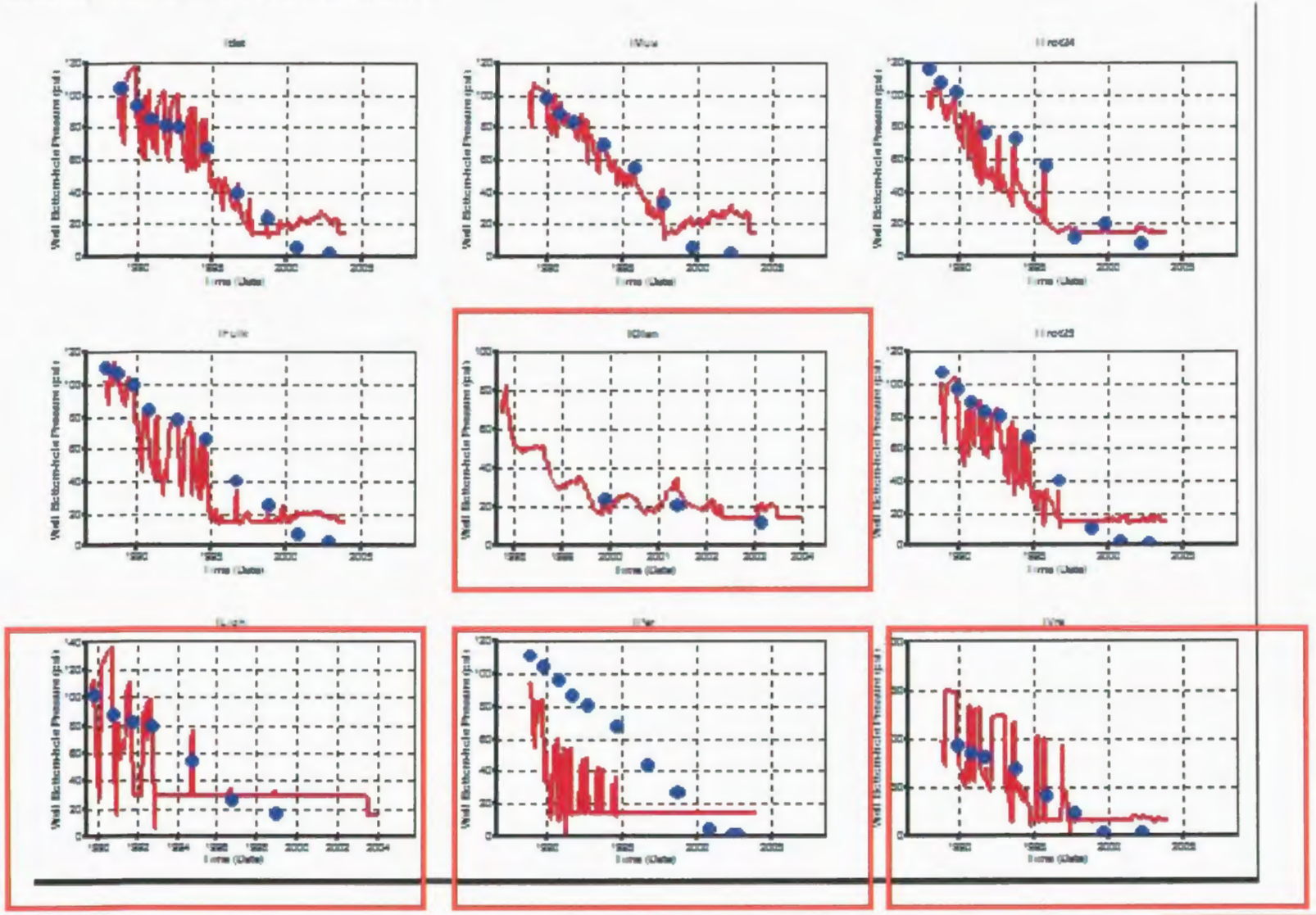

Red broken line – Sim bottom hole pressure (BHP flowing), Blue circles – Well head flowing pressure (WHFP). Border wells

Figure 4.6.6

6th Run – Pi = 423 psi, OGIP = 179.5 bcf.

Res Pr distribution as of Jan 1, 1970 – before CG wells

CG Fractures extend to L2 & Pi = 423 psi

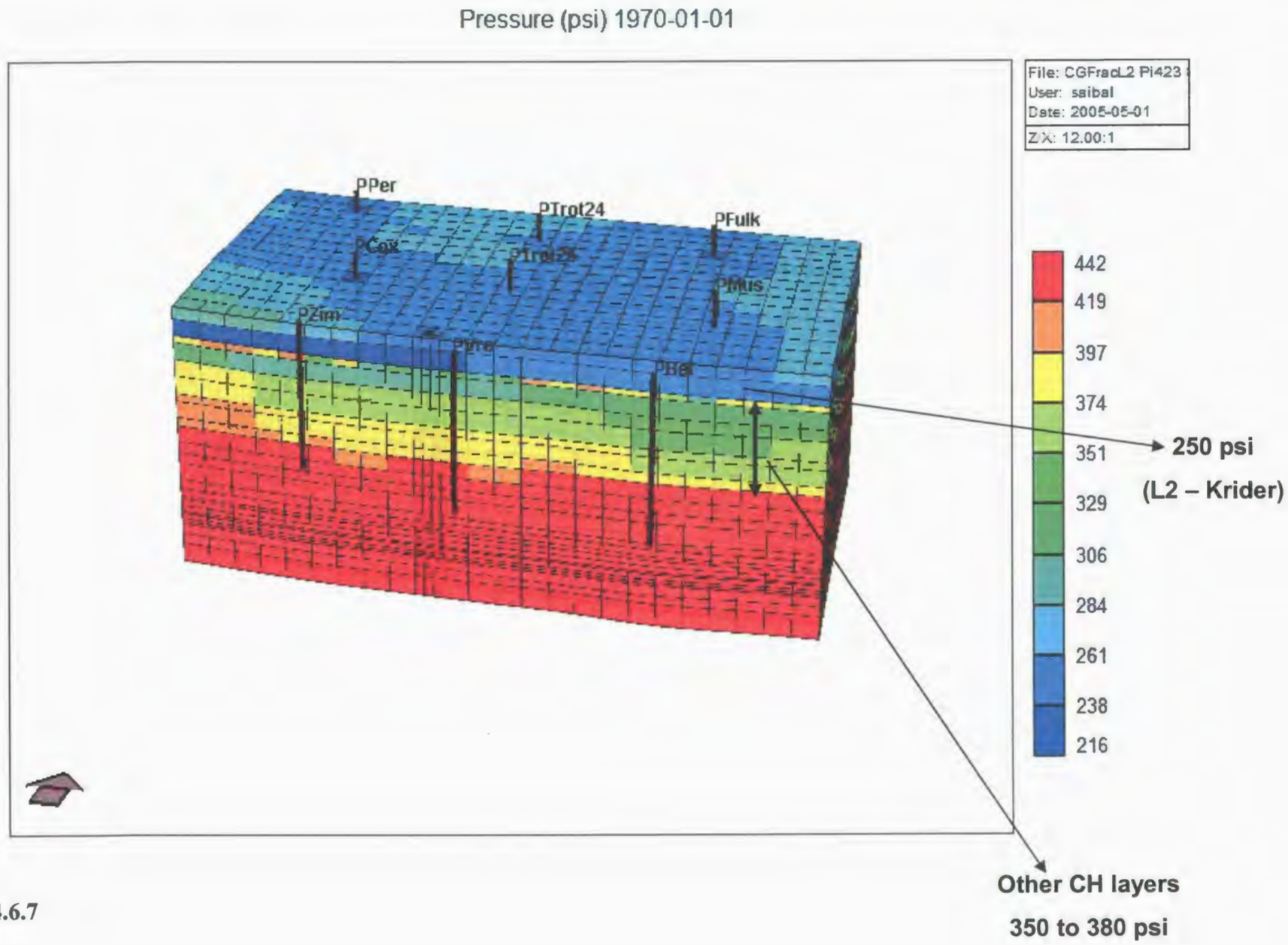

Figure 4.6.7

6th Run – Pi = 423 psi, OGIP = 179.5 bcf.

A.

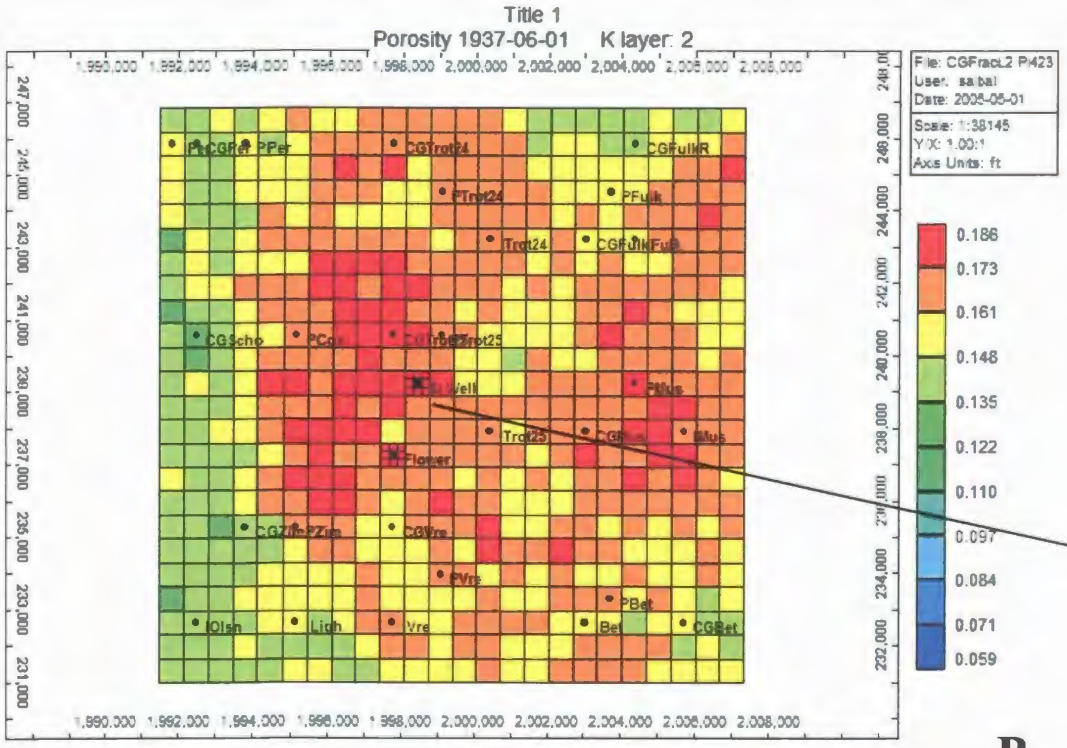

All CG wells in the model have ff ranging between 5 and 9.

Thus, to test what kind of shut in pressure could be obtained from a CG well before significant production, a hypothetical CG well ("SI Well") was located just north of the Flower well and shut-in tests were carried out on this well.

Located a Test well called "SI Well". Completed on Jan 1, 1970. Well located within a mesh of refined grids.

SI Well Completed from L2 to L23.

SI Well not fractured (ff=1).

SI Well flowed for 1 day.

Well shut in on Jan 2, 1970.

SI pressure stabilizes around 238 psi after 72 hrs. This is close to what has been typically recorded at CG wells upon completion in the study area.

SI pr at a hypothetical CG well – Jan 1970

B.

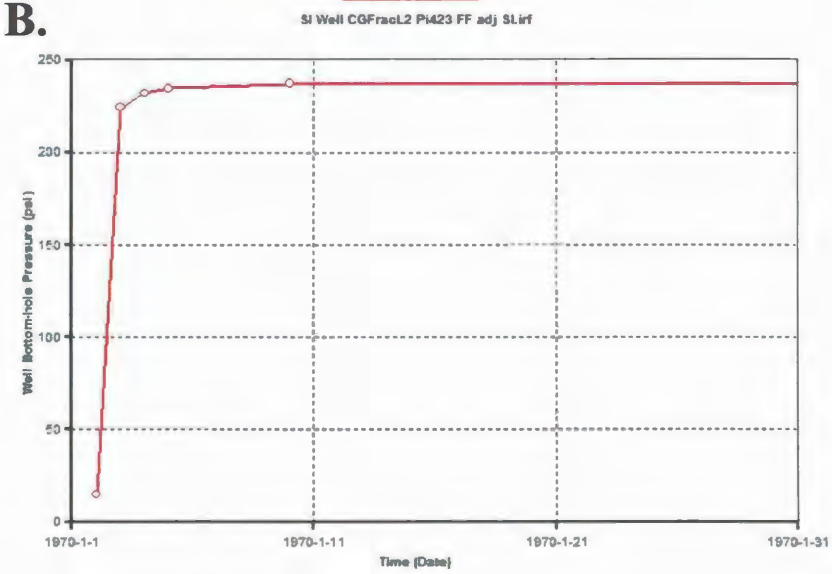

Figure 4.6.8

6th Run – Pi = 423 psi, OGIP = 179.5 bcf.

Res Pr distribution as of Jan 1, 1995 – Flower test date

CG Fractures extend to L2 & Pi = 423 psi

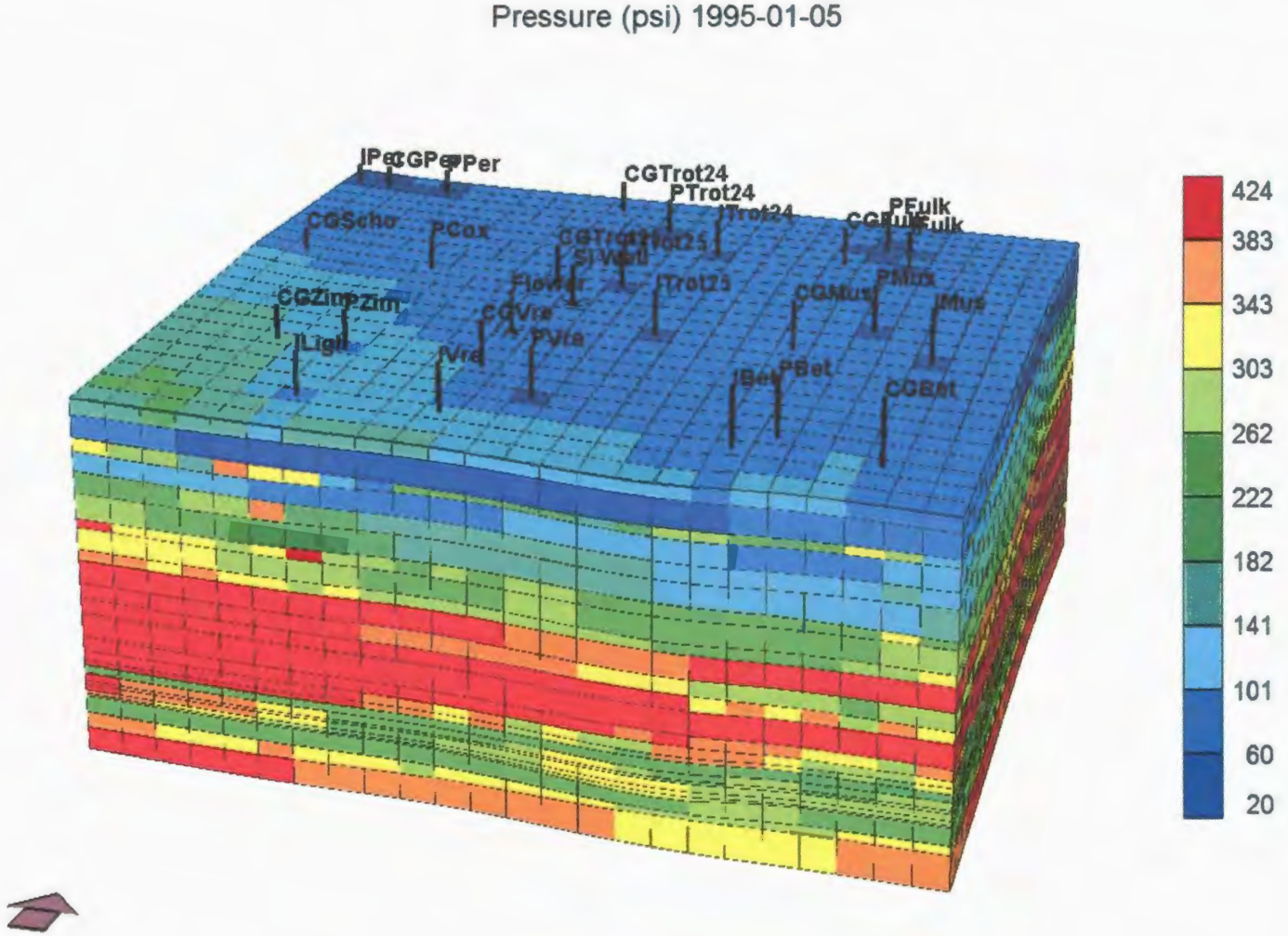

Figure 4.6.9

Compare Layer DST data at Flower on Jan 5, 1995

6th Run – Pi = 423 psi, OGIP = 179.5 bcf.

A.

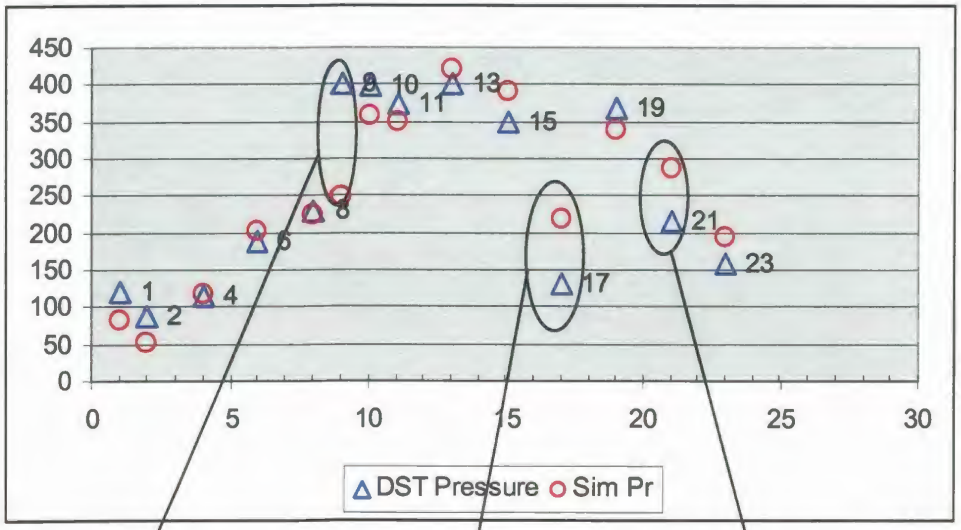

Layer 9 – L/FTRLY

Layer 17 – B2LM

Layer 21 – B4LM

Close matches obtained in most layers except L/FTRLY, B2LM and B4LM where the simulator calculated pressures are significantly higher than that recorded in Flower DSTs. It appears that despite matching CG production histories, layers such as B2LM and B4LM have not drained to the extent that the Flower DSTs indicate.

Is gas being drained from these layers by non-CG wells?

The only possible candidates are CH P and I wells.

May be hydraulic fractures in CH wells went into CG.

So next few simulator runs will have fractures in CH (P&I) wells extend to L23 along with CG fractures extending to L2 (as before).

B.

As of Jan 5, 1995
CG frac L2
All ff adj
Pi = 423 psi

	Layer	DST	Sim Pr
1 Hrngtn-Paddock	1	120.3	81
2 Krider	2	87.9	53
3 Odell	3		
Wnf SS			
4 Wnf LS	4	113.4	116
5 Gage	5		
6 Towanda	6	187.0	201
7 B/TWND	7		
8 FTRLY	8	229.9	224.4
9 L/FTRLY	9	400.0	249
10 B/FTRLY	10	398.4	356
11 WREFORD	11	372.4	350
12 A1_SH	12		
13 A1_LM	13	400.0	420
14 B1_SH	14		
15 B1_LM	15	350.0	389
16 B2_SH	16		
17 B2_LM	17	130.6	217
18 B3_SH	18		
19 B3_LM	19	368.0	339
20 B4_SH	20		
21 B4_LM	21	215.0	286
22 B5_SH	22		
23 B5_LM	23	159.5	194
24 C_SH	24		
25 C_LM	25		

Figure 4.6.10

SI pr at a hypothetical CG well – Jan 1970

7th Run – Pi = 423 psi, OGIP = 179.5 bcf.

CH well (P&I) fractures extended to L23 and CG fractures go to L2

FF factors unchanged from 6th Run

Production and pressure matches at CH wells (P&I) and CG wells remain largely unchanged.

A.

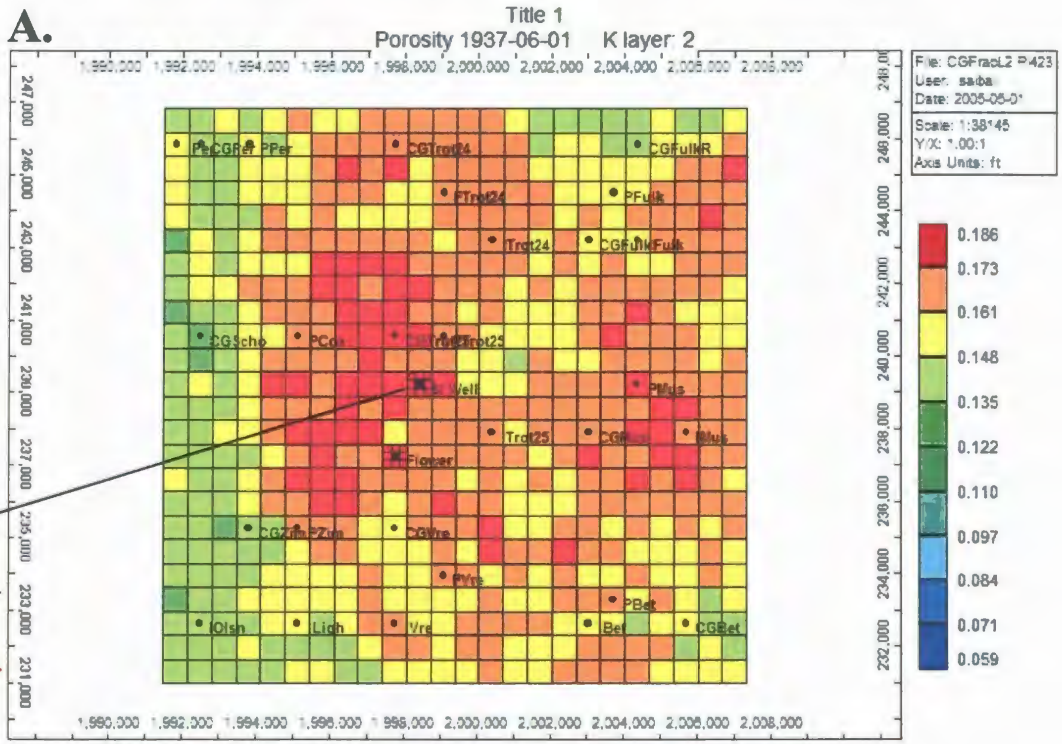

B.

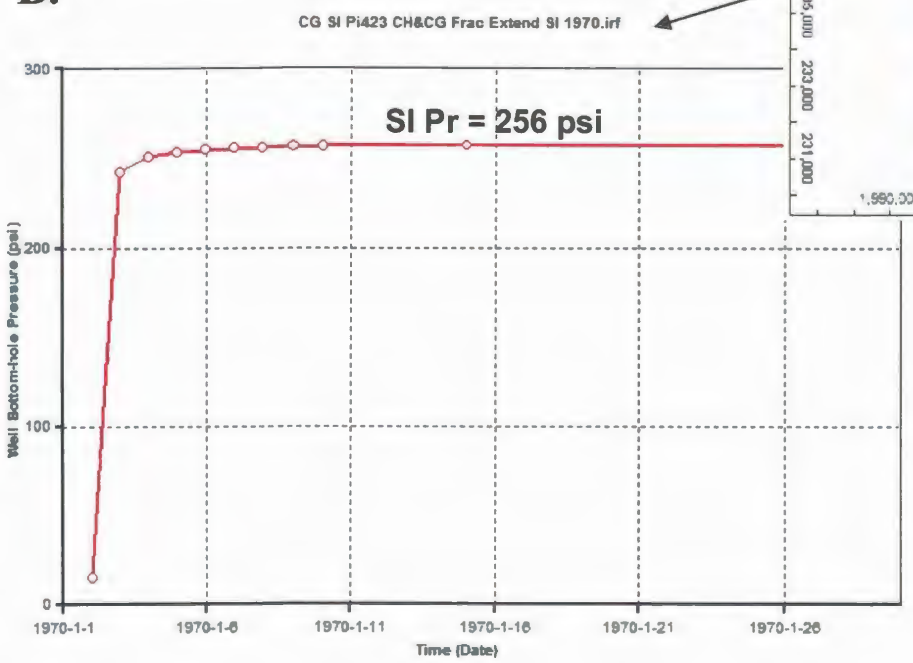

Extending CH fractures into CG enables getting slightly higher SI pressures at CG wells upon completion. This higher SI value is more closer to 265 psi – the pressure that has recorded at CG wells, than that obtained in 6th Run.

Figure 4.7.1

7th Run – Pi = 423 psi, OGIP = 179.5 bcf.

CH well (P&I) fractures extended to L23 and CG fractures go to L2

FF factors unchanged from 6th Run

Compare Layer DST data at Flower on Jan 5, 1995

A.

	Layer	DST	Run 6 As of Jan 5, 1995 CG frac L2 All ff adj Pi = 423 psi Sim Pr	Run 7 FF same as before CH frac to CG CG ff to CH Pi = 423 psi Frac Ext
1 Hrngtn-Paddock	1	120.3	81	93.6
2 Krider	2	87.9	53	64
3 Odell Wnf SS	3			
4 Wnf LS	4	113.4	116	126.9
5 Gage	5			
6 Towanda	6	187.0	201	212.1
7 B/TWND	7			
8 FTRLY	8	229.9	224.4	232.2
9 L/FTRLY	9	400.0	249	255.2
10 B/FTRLY	10	398.4	356	347.7
11 WREFORD	11	372.4	350	320.3
12 A1_SH	12			
13 A1_LM	13	400.0	420	419.7
14 B1_SH	14			
15 B1_LM	15	350.0	389	371
16 B2_SH	16			
17 B2_LM	17	130.6	217	149
18 B3_SH	18			
19 B3_LM	19	368.0	339	308.4
20 B4_SH	20			
21 B4_LM	21	215.0	286	250.3
22 B5_SH	22			
23 B5_LM	23	159.5	194	131
24 C_SH	24			
25 C_LM	25			

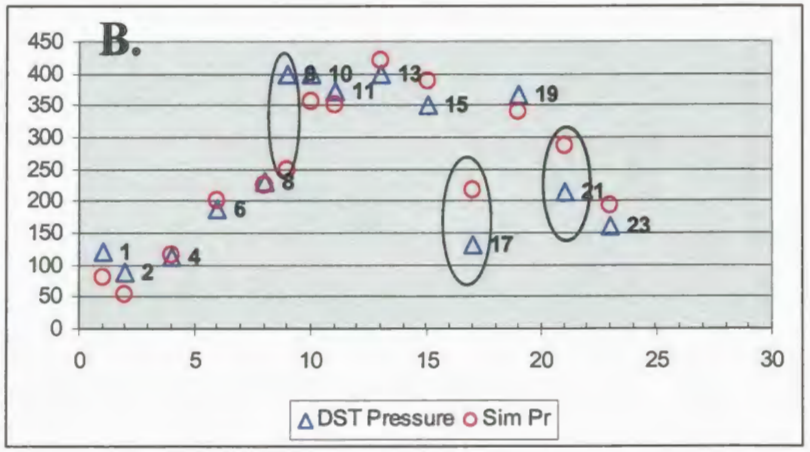

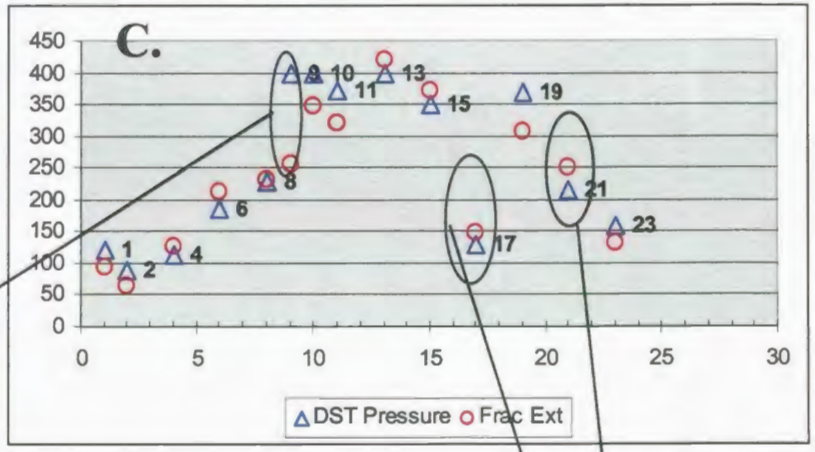

Layer 9 is L/FrtRly – simulator calculates a lower pressure at this zone

Pressure matches improve in Layers 17 and 21 when CH completions extended in CG

Figure 4.7.2

7th Run – Pi = 423 psi, OGIP = 179.5 bcf.

CH well (P&I) fractures extended to L23 and CG fractures go to L2

FF factors unchanged from 6th Run

			Run 6	Run 7	
				As of Jan 5, 1995	As of Jan 1, 2004
			As of Jan 5, 1995	FF same as befor	FF same as befor
			CG frac L2	CH frac to CG	CH frac to CG
			All ff adj	CG ff to CH	CG ff to CH
			Pi = 423 psi	Pi = 423 psi	Pi = 423 psi
	Layer	DST	Sim Pr	Sim Output	Sim Output
Hrngtn-Paddock	1	120.3	81	93.6	54.8
Krider	2	87.9	53	64	27.8
Odell	3		113	124	78.6
Wnf SS		105.4*			
Wnf LS	4	121.4	116	126.9	81.7
Gage	5	NO TEST	201	211.5	168.9
Towanda	6	187.0	201	212.1	165.1
B/TWND	7	NO TEST	219.5	227.4	180.8
FTRLY	8	229.9	224.4	232.2	185.2
L/FTRLY	9	>400.0	249	255.2	213.5
B/FTRLY	10	398.4	356	347.7	315.9
WREFORD	11	372.4	350	320.3	278.7
A1_SH	12	NO TEST	418	417	414.1
A1_LM	13	400.0	420	419.7	417.1
B1_SH	14	NO TEST	419.8	418.2	415.2
B1_LM	15	350.0	389	371	351.3
B2_SH	16	NO TEST	387	369	349.5
B2_LM	17	130.6	217	149	101.2
B3_SH	18	NO TEST	338	307	278.1
B3_LM	19	368.0	339	308.4	279.2
B4_SH	20	NO TEST	338	307.9	278.7
B4_LM	21	215.0	286	250.3	214.8
B5_SH	22	NO TEST	287	251	214.8
B5_LM	23	159.5	194	131	85.6
C_SH	24	NO TEST	342	321.2	302.1
C_LM	25	NO TEST	409	403	393.5

Figure 4.7.3

7th Run – Pi = 423 psi, OGIP = 179.5 bcf.

CH well (P&I) fractures extended to L23 and CG fractures go to L2

FF factors unchanged from 6th Run

Compare layer pressures at Flower – Jan 1995 and Jan 2004

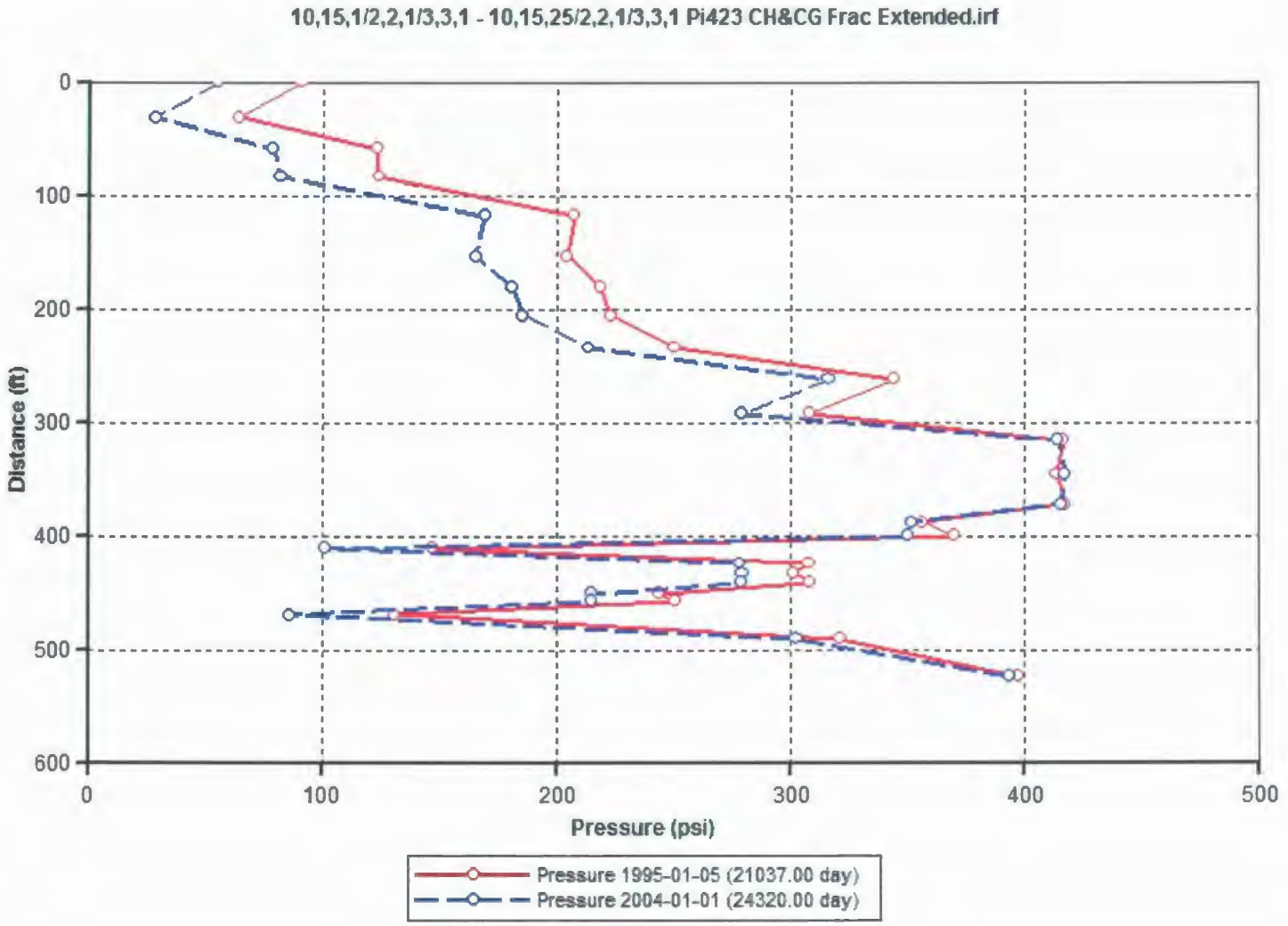

Figure 4.7.4

7th Run – Pi = 423 psi, OGIP = 179.5 bcf.

CH well (P&I) fractures extended to L23 and CG fractures go to L2

FF factors unchanged from 6th Run

Pressure distribution as of Jan 2004 – end of the simulation time period

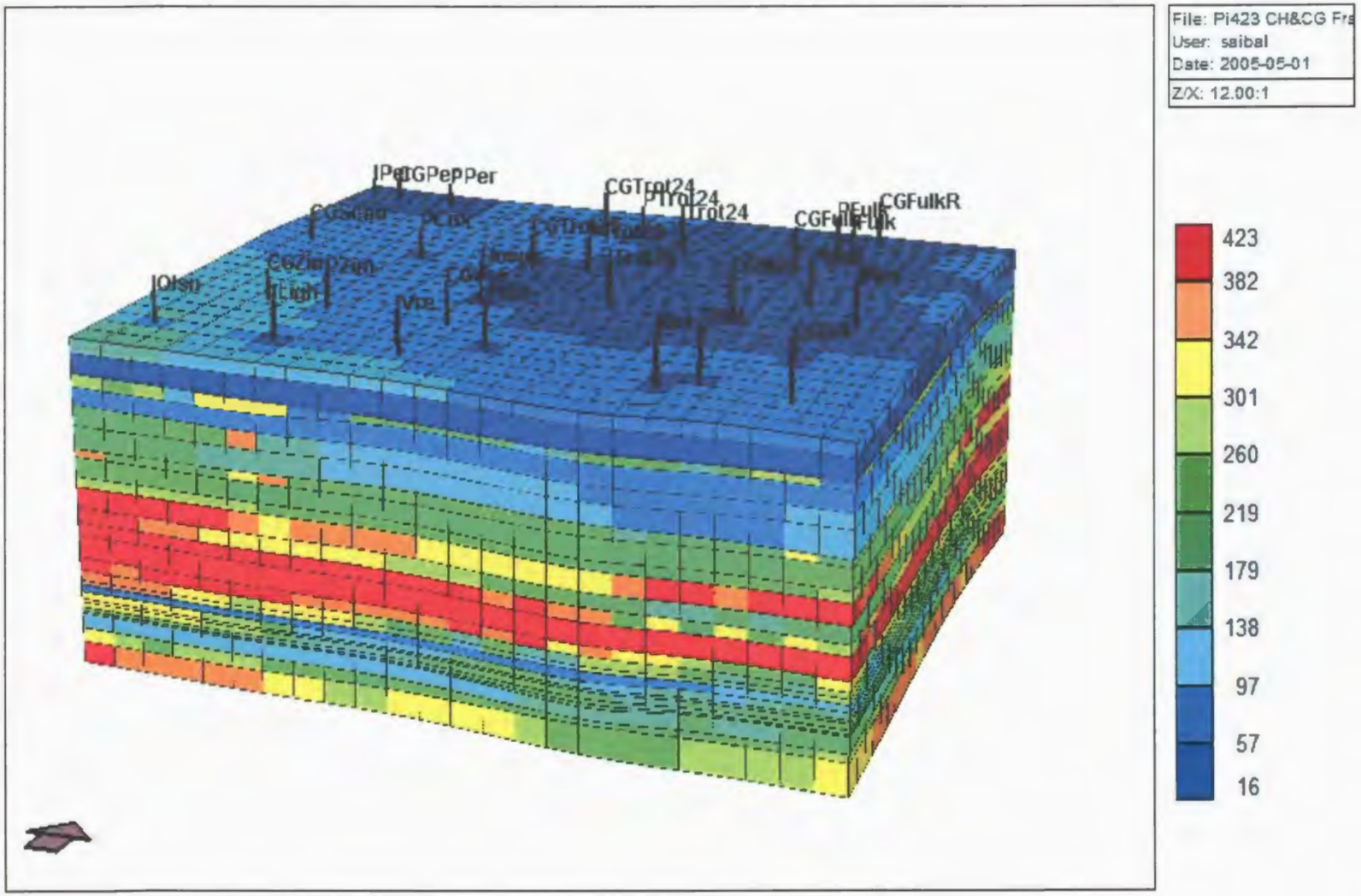

Figure 4.7.5

8th Run – Pi = 423 psi, OGIP = 179.5 bcf.

CH well (P&I) fractures extended through L17 and CG fractures go to L8

FF factors unchanged from 6th Run

A What happens if CH completions extended to B2LM and CG completions went up to Fort Rly?

CG Prod matches displayed

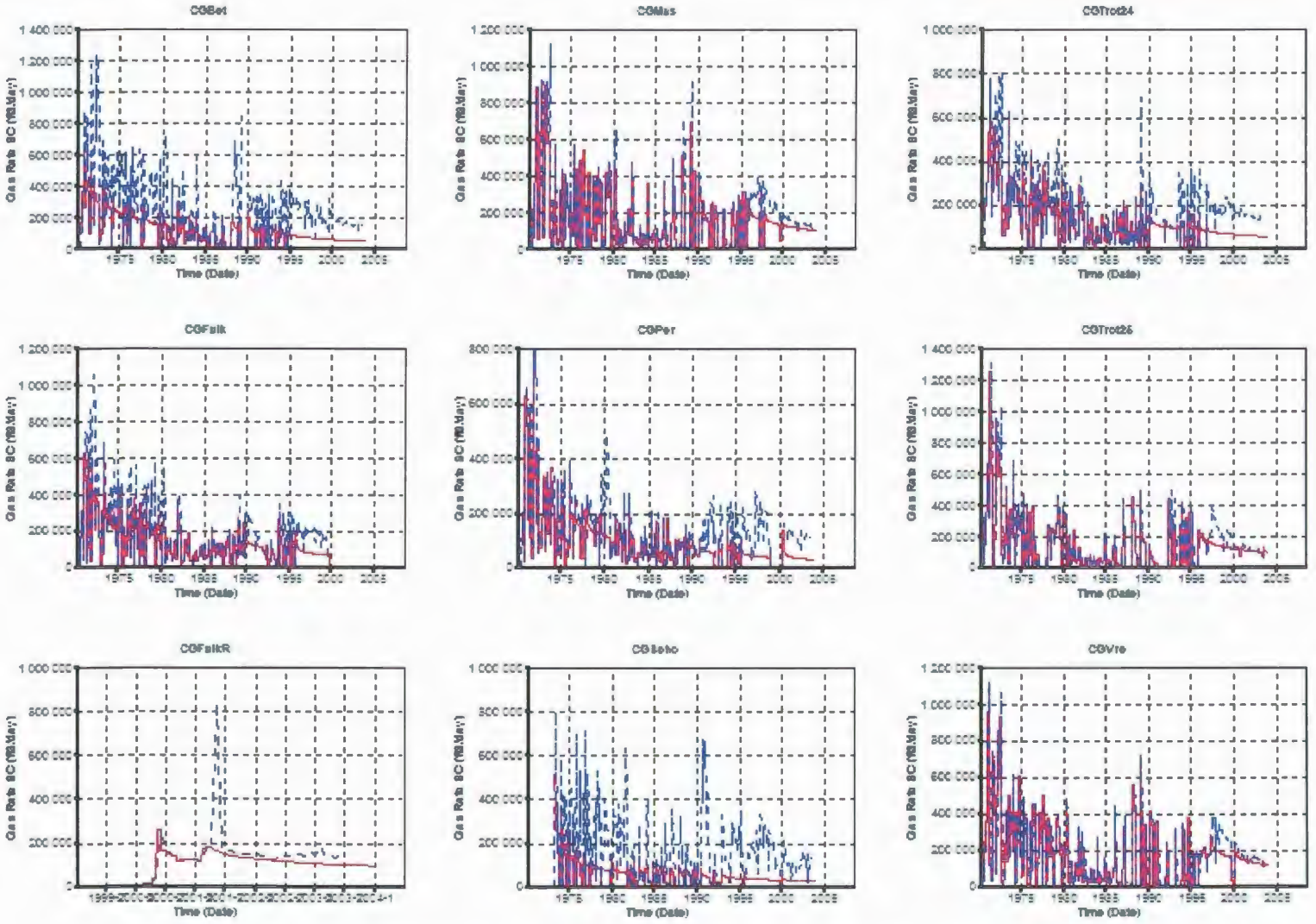

Red line – Simulator (Sim) calculated gas rate, Blue broken line – historic gas production

Figure 4.8.1

8th Run – Pi = 423 psi, OGIP = 179.5 bcf.

CH well (P&I) fractures extended through L17 and CG fractures go to L8

FF factors unchanged from 6th Run

Compare layer pressures at Flower – Run 7 & Run 8

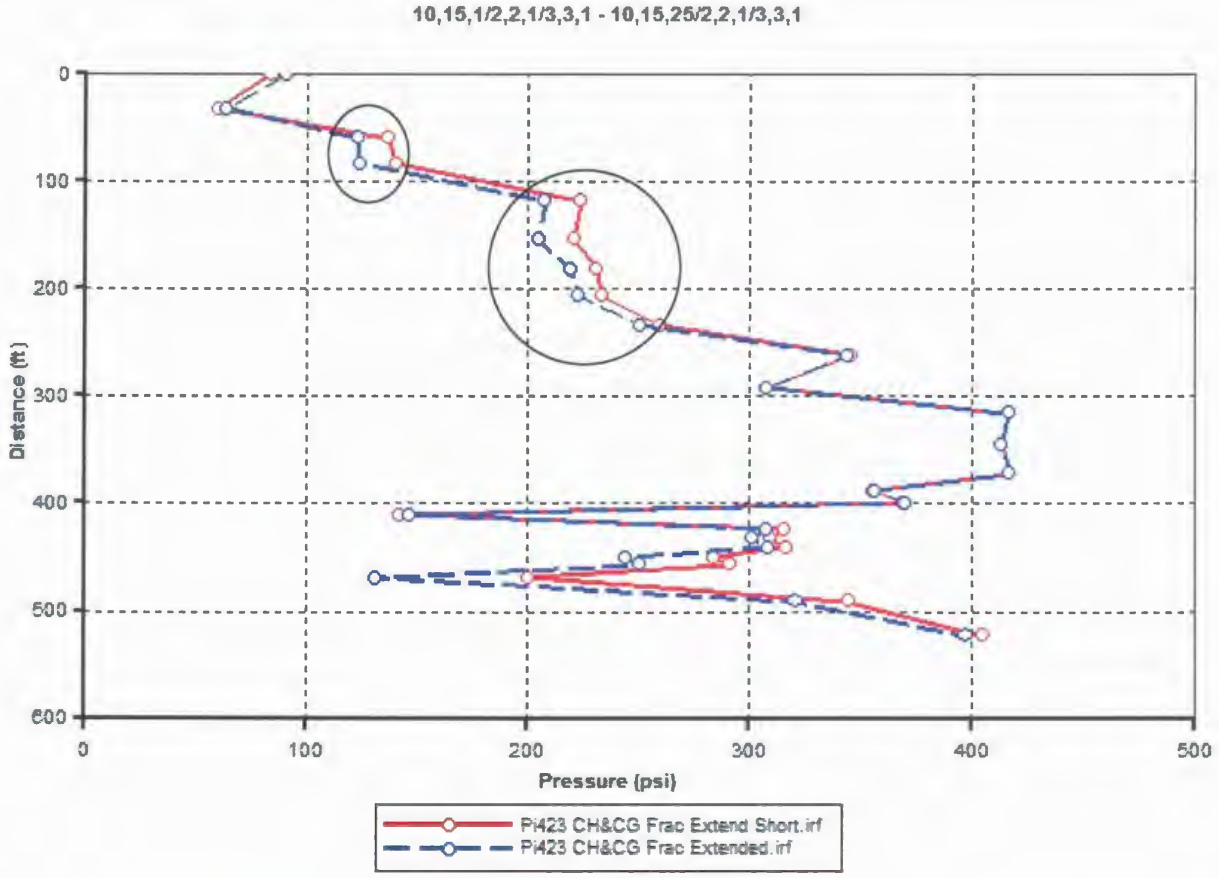

Blue line - represents Run 7. Red line - represents Run 8.

Figure 4.8.2